

## DATA NOTE

REVISED

# MIST: A multi-resolution parcellation of functional brain networks [version 2; peer review: 4 approved]

Sebastian Urchs 1,2, Jonathan Armoza<sup>2,3</sup>, Clara Moreau<sup>2,4</sup>, Yassine Benhajali<sup>2</sup>, Jolène St-Aubin<sup>2</sup>, Pierre Orban<sup>2,5,6</sup>, Pierre Bellec<sup>2,7</sup>

<sup>1</sup>Montreal Neurological Institute, McGill University, Montreal, QC, H3A 2B4, Canada

<sup>2</sup>Centre de recherche de l'Institut universitaire de gériatrie de Montréal, Montreal, QC, H3W 1W5, Canada

<sup>3</sup>Department of English, New York University, New York, NY, 10003, USA

<sup>4</sup>Centre hospitalier universitaire Sainte-Justine, Montreal, QC, QC H3T 1C5, Canada

<sup>5</sup>Centre de recherche de l'Institut universitaire de santé mentale de Montréal, Montreal, QC, H1N 3M5, Canada

<sup>6</sup>Département de psychiatrie, Université de Montréal, Montreal, QC, H3T 1J4, USA

<sup>7</sup>Département d'informatique et recherche opérationnelle, Université de Montréal, Montreal, QC, H3T 1J4, Canada

**V2** First published: 05 Dec 2017, 1:3 (  
<https://doi.org/10.12688/mnior.12767.1>)

Latest published: 05 Mar 2019, 1:3 (  
<https://doi.org/10.12688/mnior.12767.2>)

## Abstract

The functional architecture of the brain is organized across multiple levels of spatial resolutions, from distributed networks to the localized areas they are made of. A brain parcellation that defines functional nodes at multiple resolutions is required to investigate the functional connectome across these scales. Here we present the Multiresolution Intrinsic Segmentation Template (MIST), a multi-resolution group level parcellation of the cortical, subcortical and cerebellar gray matter. The individual MIST parcellations match other published group parcellations in internal homogeneity and reproducibility and perform very well in real-world application benchmarks. In addition, the MIST parcellations are fully annotated and provide a hierarchical decomposition of functional brain networks across nine resolutions (7 to 444 functional parcels). We hope that the MIST parcellation will accelerate research in brain connectivity across resolutions. Because visualizing multiresolution parcellations is challenging, we provide an [interactive web interface](#) to explore the MIST. The MIST is also available through the popular [nilearn](#) toolbox.

## Keywords

brain parcellation, functional connectivity, stable networks, hierarchical organization, nodes, graph, brain segmentation

## Open Peer Review

Reviewer Status

	Invited Reviewers			
	1	2	3	4
version 2 (revision) 05 Mar 2019	 report		 report	
version 1 05 Dec 2017	 report	 report	 report	 report

1 **Lucina Q. Uddin** , University of Miami, Miami, USA

2 **Vinod Menon**, Stanford University, Stanford, USA

3 **Clare Kelly** , Trinity College Dublin, Dublin, Ireland

4 **Darya Chyzyk** , INRIA, Paris-Saclay, Paris, France

Any reports and responses or comments on the article can be found at the end of the article.

**Corresponding authors:** Sebastian Urchs ([sebastian.urchs@gmail.com](mailto:sebastian.urchs@gmail.com)), Pierre Bellec ([pierre.bellec@criugm.qc.ca](mailto:pierre.bellec@criugm.qc.ca))

**Author roles:** **Urchs S:** Data Curation, Formal Analysis, Investigation, Resources, Validation, Visualization, Writing – Original Draft Preparation, Writing – Review & Editing; **Armoza J:** Visualization, Writing – Review & Editing; **Moreau C:** Data Curation; **Benhajali Y:** Data Curation, Writing – Review & Editing; **St-Aubin J:** Visualization, Writing – Review & Editing; **Orban P:** Writing – Review & Editing; **Bellec P:** Conceptualization, Funding Acquisition, Methodology, Project Administration, Resources, Software, Supervision, Writing – Review & Editing

**Competing interests:** No competing interests were disclosed.

**Grant information:** This work was supported by grants from Brain Canada (JA, JSA), Brain Canada (SU, CM), Azrieli foundation (SU), and Natural Sciences and Engineering Research Council (YB), as well as a salary award by Fonds de Recherche du Québec - Santé (FRQS) and the Courtois foundation to PB.

**Copyright:** © 2019 Urchs S *et al.* This is an open access article distributed under the terms of the [Creative Commons Attribution License](#), which permits unrestricted use, distribution, and reproduction in any medium, provided the original work is properly cited.

**How to cite this article:** Urchs S, Armoza J, Moreau C *et al.* **MIST: A multi-resolution parcellation of functional brain networks [version 2; peer review: 4 approved]** MNI Open Research 2019, 1:3 (<https://doi.org/10.12688/mniopenres.12767.2>)

**First published:** 05 Dec 2017, 1:3 (<https://doi.org/10.12688/mniopenres.12767.1>)

**REVISED Amendments from Version 1**

In the updated version of this article, we have clarified how the MIST parcellation addresses the need for an annotated, multi-resolution brain parcellation. We compare the quality, replicability, and generalizability of the individual MIST parcellations in more detail to widely used parcellations in the field. To compute the out of sample reproducibility of our parcellation we have included data from the Genomics Superstruct Project. These data were prepared by Clara Moreau who has been added to the author's list. [Figure 9](#) has been added to illustrate the results of the replicability analysis. We provide a more detailed comparison of the MIST parcellation to existing brain parcellations, in particular the Yeo and Glasser parcellations. [Figure 5](#) and [Figure 6](#) have been added to illustrate these results while the previous [Figure 5](#) and [Figure 6](#) have been renumbered [Figure 7](#) and [Figure 8](#), respectively. We have extended our discussion of these comparisons and emphasize that while the MIST parcellation matches existing parcellations in metrics of reproducibility and generalizability, it adds unique functionality not otherwise available.

**See referee reports**

## Introduction

Understanding the building blocks of the human brain is a long-standing goal of neuroscience. An early and important example is the parcellation of the brain into distinct areas of homogeneous cytoarchitecture by Korbinian Brodmann at the beginning of last century<sup>1</sup>. This line of work has since been extended to include brain parcellations based on a range of brain modalities, such as sulcal landmarks<sup>2</sup>, functional connectivity<sup>3</sup>, task activation<sup>4</sup>, gene expression patterns<sup>5</sup>, and combinations of different imaging modalities<sup>6</sup>. Good parcellations generate homogeneous parcels that tell us something about the organization of the brain along the corresponding modality, provide a common frame of reference for the localization of new findings, and serve the additional purpose of meaningful dimensionality reduction<sup>7,8</sup>.

Analyzing functional connectivity at very high spatial resolutions, e.g. voxels, is neither practical nor informative for most applications<sup>9,10</sup>. Connectivity is instead often estimated at the level of larger brain regions or networks that are delineated by a brain parcellation, thus providing an informed way of spatial dimensionality reduction. Brain parcellations based on resting-state functional magnetic resonance imaging (rsfMRI) have been shown to better summarize the whole-brain connectivity than parcellations based on histological or anatomical features<sup>7</sup> and are therefore a reasonable choice for investigations of functional connectivity.

Researchers can choose from a wide range of functional brain parcellations in the literature that are generated using different algorithms<sup>10,11</sup> and datasets, and provide parcels at different spatial resolutions and in different reference spaces. Spatial resolution in particular is an important difference between brain parcellations. The organization of the functional brain can be understood as a hierarchy of functional modules that spans from few, large, and distributed functional networks to many, small, and locally integrated functional areas. There are about 5–15 canonical

whole-brain functional networks<sup>8</sup> and a widely used parcellation at that resolution is the surface atlas generated by Yeo and colleagues<sup>3</sup>. The other end of the spatial resolution spectrum is less clearly defined. Resolutions between 200<sup>7,12</sup> and 400<sup>11,13</sup> whole-brain parcels are commonly considered to reflect functional areas. A good example of a functional area parcellation is the comprehensive surface atlas by Glasser and colleagues that defines functional areas separated by consensus boundaries across functional and anatomical imaging modalities<sup>6</sup>. Resolutions beyond 400 whole-brain parcels generally reflect functional atoms that are very small, spatially contiguous clusters within one or two orders of magnitude of the resolution of the data<sup>7,14</sup>.

Which spatial resolution to choose among this wide range of available resolutions will depend on the spatial scale of the investigated effect. For a systems level research question, a low resolution parcellation of large scale functional networks may be appropriate whereas a high resolution functional area parcellation will be better suited to define the nodes in a full connectome model. For each target spatial scale, several parcellations may be suitable depending on the preferred parcellation coverage (neo-cortex, cerebellum, subcortical areas), and space (surface, volumetric).

Choosing the right parcellation is more challenging if several effects with different spatial scales are investigated or one effect is investigated across several spatial resolutions<sup>15–17</sup>. Different parcellations can be used for different spatial resolutions, but this is typically not desirable if there are significant methodological differences between parcellations and they may have been derived from different datasets. An alternative is to use one of the published automatic or semi-automatic parcellation algorithms to generate data-specific brain parcellations at the desired scales. This addresses the methodological confounds but makes the results harder to compare or reproduce across different studies. In addition, generating and testing a new brain parcellation is typically quite laborious which makes it an infeasible solution for data exploration. A third solution is therefore to use a multi-resolution brain parcellation that covers the desired spatial resolutions.

To the best of our knowledge, only three existing parcellations provide functional connectivity based multi-resolution parcellations<sup>7,12,14</sup>. The MIST parcellation differs from these parcellations in two key aspects: 1) existing parcellations aim to define functional areas and therefore focus on higher spatial resolutions (>100 parcels) than the MIST parcellation (>7 parcels) which aims to provide a decomposition of functional networks. 2) the MIST parcellation provides annotated parcels embedded in a hierarchical decomposition tree that have no equivalent in existing multi-resolution parcellations. For a more in depth discussion of the differences between existing brain parcellations and the MIST parcellation please refer to the section on Comparison with existing atlases.

We have generated the MIST atlas with the goal to address the need for an annotated multi-resolution decomposition of large functional networks into functional areas. We have based our

atlas on a high quality dataset and an extensively tested algorithm for the extraction of stable group level parcellations<sup>18</sup>. The MIST atlas provides brain parcels in MNI152 space for spatial resolutions ranging from large functional networks (7) to individual functional areas (444). Importantly, the volumetric parcels of the MIST atlas cover the entire brain, that is cortical, subcortical and cerebellar gray matter. We have further manually labeled all parcellations up to a spatial resolution of 122 and have automatically labeled parcellations of higher resolutions. Lastly, we found that parcellations across spatial resolutions, while derived separately from the data, strongly align along a hierarchical decomposition tree. We therefore provide a hierarchical ordering of brain parcels across spatial resolutions to assist in cross-resolution investigations.

The MIST atlas is freely available to the public through our data repository and the nilearn analysis package ([nilearn.github.io](https://nilearn.github.io))<sup>19</sup>. The individual brain parcellations included in the MIST atlas have previously been made available for download on figshare<sup>20</sup>. These individual parcellations are identical to the individual MIST parcellations. The aim of this work is to provide a comprehensive description of the methodology used to create the MIST atlas and to facilitate its use by providing descriptive labels for the parcellations, the empirically derived hierarchical decomposition, and our interactive exploration tool. We hope that this contribution will facilitate cross-resolution research of the functional brain.

## Methods

### Sample

All data were taken from the publicly available Cambridge dataset<sup>21</sup>, which is available from the 1000 functional connectomes project<sup>22</sup>. The Cambridge dataset consists of 198 subjects (123 female) between 18 and 30 years of age. Six minutes of rs-fMRI data (TR=3s, 119 time points) were recorded on a 3 Tesla Siemens Tim Trio Scanner (Siemens Medical Systems, Erlangen, Germany) at 3s TR using a 12-channel head coil. We have chosen this dataset due to the high quality of the imaging data, the low degree of in-scanner motion among individuals in the dataset, and because the acquisition parameters are representative of the average functional imaging study in the field in terms of spatial resolution and length of the scan. The sample is also shared without any access restrictions and has a moderate size, making it easy for other groups to attempt a replication or extension of our work.

### Preprocessing

The data were preprocessed using the Neuroimaging Analysis Kit (NIAK) version 0.12.4<sup>23</sup>, an Octave<sup>24</sup> based open source processing and analysis framework for imaging data. Each individual data set was corrected for differences in slice acquisition time. Head motion parameters were estimated by spatially re-aligning individual time points with the median volume in the series. This reference median volume was then aligned with the anatomical T1 image of the individual which in turn was coregistered onto the MNI152 template space<sup>25</sup> using an initial affine transformation followed by a nonlinear

transformation. Finally, each individual time point was mapped to MNI152 space using the combined spatial transformations. For time points with excessive in scanner motion (> 0.5mm framewise displacement), the time point as well as the preceding and the two following time points were removed from the time series<sup>26</sup>. Nuisance covariates were regressed from the remaining time series: slow time drifts (basis of discrete cosines with a 0.01 Hz high-pass cut-off), average signals in conservative masks of the white matter and the lateral ventricles as well as the first principal components (95% energy) of the six rigid-body motion parameters and their squares<sup>27,28</sup>. Data were then spatially smoothed with a 3D gaussian kernel (FWHM = 6mm).

### Quality control

The quality of the registration operations was visually inspected following an in-house developed quality control protocol<sup>29</sup>. Specifically the registration between the individual T1 scans and the stereotaxic template space, as well as registration between the individual T1 and the median functional image were assessed. Subjects were excluded from the analysis in cases of failed coregistration with the template space or where less than 40 time points had acceptable amounts of head motion after scrubbing. A total of 190 subjects (119 female, mean age 21 years, SD 2.3) passed quality control criteria for inclusion in the analysis.

### Generating the MIST parcellation

Functional connectivity was computed as the fisher-z transformed Pearson correlation between time series. Stable networks of functional connectivity were extracted from rsfMRI data using an implementation of the Bootstrap Analysis of Stable Clusters (BASC) algorithm<sup>18</sup> within NIAK. The goal of the BASC process is to identify groups of brain regions that exhibit consistent and strong functional connectivity at the individual and group level. In brief, the process consists of three stages:

First, we apply a dimensionality reduction procedure using a region growing algorithm<sup>30</sup>. The algorithm iteratively merges spatially contiguous voxels with highly correlated time series to form 1095 functional atoms (part of the release as MIST\_ATOM). Second, we want to identify stable functional connections between these atoms at the level of individual subjects. To do so, we take 1000 bootstrap samples of the individual time series and then repeatedly cluster atoms by functional connectivity using hierarchical agglomerative clustering. We estimate how consistently two atoms are clustered together by averaging the binary adjacency matrices across bootstrap samples. This average adjacency matrix is called the individual stability matrix. Third, at the group level we want to identify connections that are consistently stable across individuals. To do so, we repeatedly sample subsets of individuals from the dataset and average their individual stability matrices. We then apply hierarchical agglomerative clustering on the average stability matrix within each subsample and binarize the resulting clustering assignment. Similar to the individual level clustering we average the binarized adjacency matrices across subsamples to obtain the group level stability matrix. Lastly, we generate the group level consensus partition on the group

level stability matrix to identify clusters of stable group level connections. A more detailed description of the method can be found in the BASC paper<sup>18</sup>.

**Selecting the resolution.** The BASC process involves decisions about the spatial resolution, i.e. the number of groups that atoms are assigned to based on the stability of their connections. These spatial resolutions must be selected for the BASC process at the individual level, at the group level, and for the final decomposition of the group stability matrix into networks. Since the stability matrices at the individual and group level are generated by clustering atoms into discrete groups they are not resolution independent, i.e. changing the number of groups will change the stability matrix. The BASC process must therefore be repeated for every combination of individual, group and network level spatial resolutions.

Our goal for the MIST parcellation was to describe stable functional networks and how they break up into smaller functional assemblies across spatial resolutions. We used the the multiscale stepwise selection algorithm (MSTEPS) to identify those spatial resolutions that best reflect major transitions in network organization across resolutions<sup>31</sup>. This process identified

nine representative group level resolutions [7, 12, 20, 36, 64, 122, 197, 325, and 444] that we included in the MIST parcellation. An additional parcellation was generated by splitting parcels of resolution 122 along the midline, which resulted in 210 fully lateralized parcels. To characterize the spatially contiguous nature of the parcels at this resolution and to distinguish it from the other parcellations we call this resolution the ‘ROI’ resolution and refer to the corresponding parcels as ROIs.

### Parcels

Figure 1 provides an overview of the functional parcels identified at the different resolutions. The first step in resolution space from 7 to 12 sees the default mode network split into 3 parts, the downstream visual areas separate from the fronto parietal network, and the auditory network and insulae separate from the ventral attention network (to explore the MIST parcellations and their decomposition across resolutions, please refer to our [interactive web viewer](#)). Beyond resolution 12, parcels begin breaking up within these large scale networks. This is illustrated by the decomposition of the somatomotor network into 3 parcels at resolution 36 and 7 parcels at resolution 122 (see Figure 2).

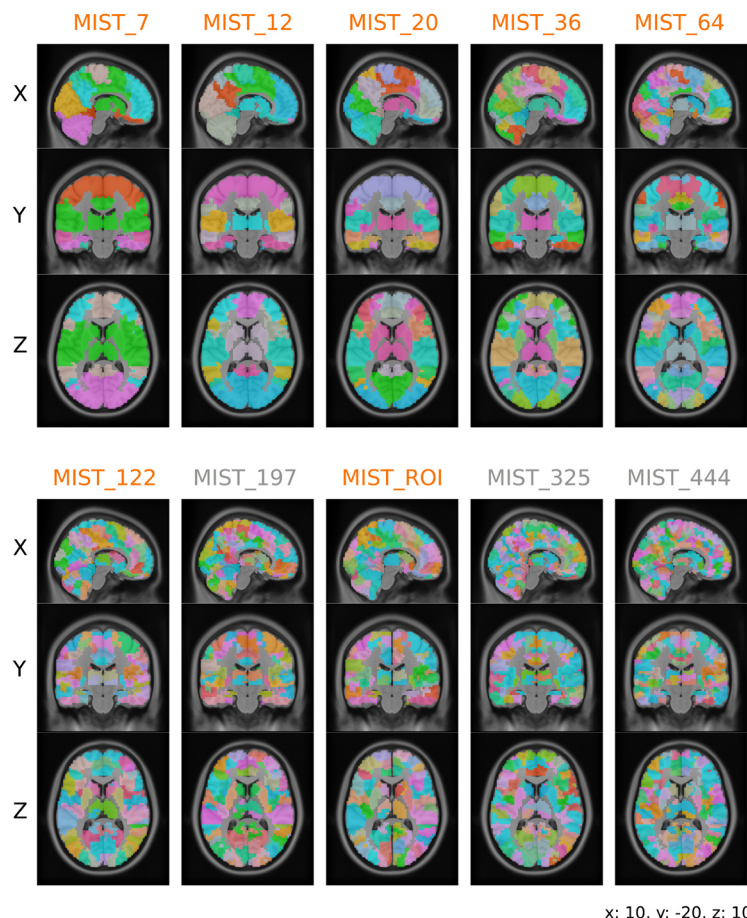


**Figure 1. Parcellation overview.** Parcellations MIST\_7 through MIST\_444 with slice coordinates denoted in MNI coordinates. Annotated parcellations are highlighted by orange parcellation names. Note that MIST\_ROI is generated by splitting MIST\_122 along the midline into fully lateralized ROIs. Parcel colors are random.

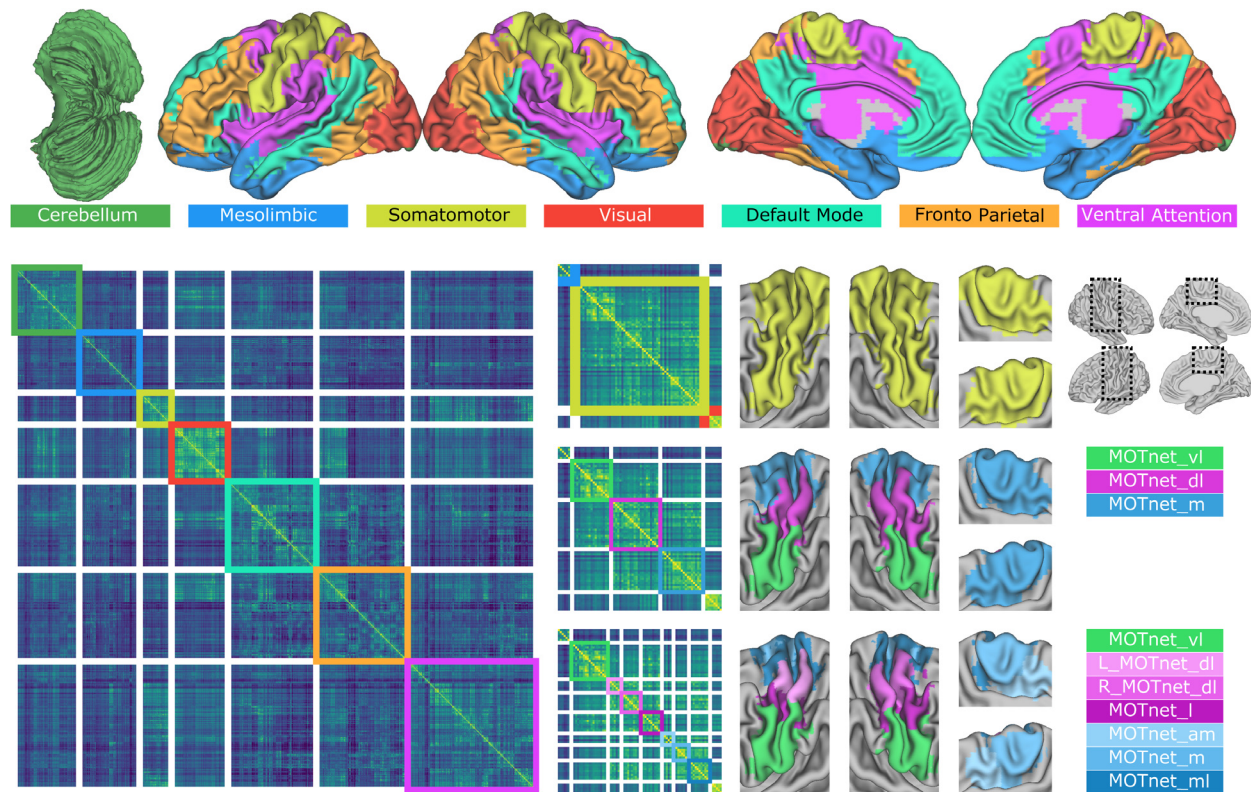


**Figure 2. Decomposition of the Somatomotor network.** (Top row) MIST\_7 rendered on the Civet<sup>32</sup> standard surface for easier visualization. (Lower left) MIST\_7 parcels highlighted over the sample-average atom by atom connectivity matrix. (Lower right) Zoomed in view on the surface and connectivity matrix representations of the Somatomotor network. Resolutions from top to bottom are: MIST\_7, MIST\_36, MIST\_122. Surface parcel colors correspond to parcels overlayed on the atom by atom connectivity matrix.

Parcels at lower resolutions are exclusively bilateral and highly symmetric, and are generally made up of spatially discontinuous subregions. These subregions tend to separate first while remaining largely bilateral. The decomposition of parcels into left- and right-hemispheric subcomponents occurs more gradually (see Figure 3). Between resolutions 36 and 64, parcels tend to become less symmetric and more lateralized. At resolution 122, from which MIST\_ROI is generated by forcing a split along the midline, more than 70% of parcels span both hemispheres. MIST\_444 has 120 parcels (or ~27% of parcels) that encompass areas in both hemispheres.

**Hierarchy.** While parcellations at each resolution have been generated independently from each other, we found that parcels at higher resolutions largely remain within the boundaries of their lower resolution parents. This allowed us to generate a pseudo-hierarchy by assigning each parcel at resolution  $R$  to the parcel at resolution  $R-1$  with the highest overlap. This pseudo-hierarchy provides a decomposition tree of large scale functional networks into fine grained functional nodes at higher resolution. The majority of parcels have an overlap of close to 100% with their parent parcels. Our web viewer gives an interactive representation of the decomposition trees for the 7 functional

networks at resolution MIST\_7. However, a subset of parcels at higher resolutions does not overlap fully with the root of the pseudo-hierarchical decomposition tree it belongs to. These parcels are predominantly located at the interface of two low resolution functional networks and may represent more ambiguous boundary regions. Figure 4 provides the overlap of parcels at all resolutions with their root parcel (the MIST\_7 parcel that the pseudo-hierarchy assigns them to). Note that we haven't included MIST\_ROI here as it is a transformation of MIST\_122 and not an independent parcellation.

**Parcel nomenclature.** Our goal in naming the functional parcels presented here was to provide an intuitive description of the general brain areas included in a parcel. Wherever appropriate, we tried to name parcels based on current terminology in the rsfMRI literature. For parcels that could not be described in their entirety by an established name, we listed the significant subcomponents of the parcel. Particularly at higher spatial resolutions, when parcels would encompass relatively small and well described areas, a functional name could sometimes not be justified. In these cases we named the parcel based on the underlying brain anatomy.

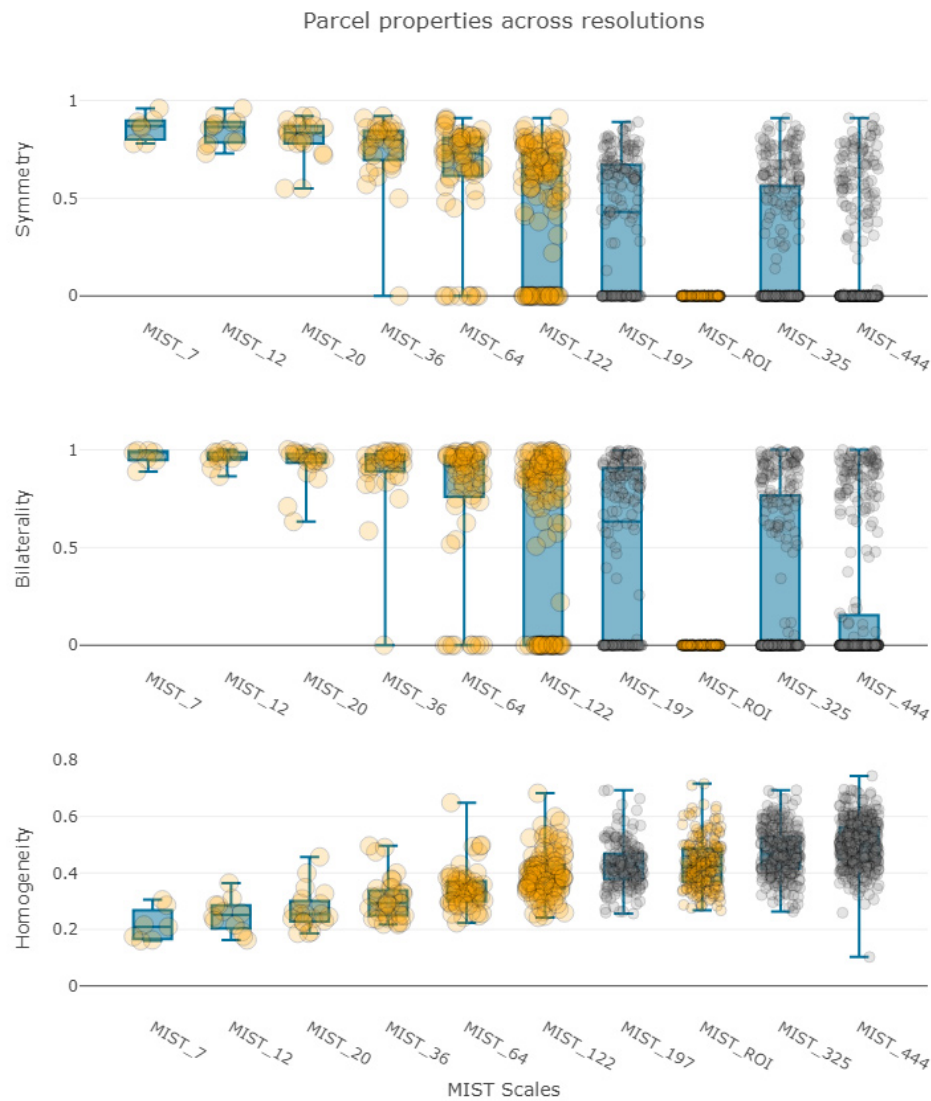


**Figure 3. Parcel properties across resolutions.** (Top row) Parcel symmetry across MIST resolutions. MIST\_ROI is the lateralized version of MIST\_122 and doesn't have symmetric parcels. (Middle row) Parcel bilaterality scores across MIST resolutions. Higher values indicate a more bilateral parcel. Bilaterality scores are computed as 1 minus the absolute value of the parcel laterality. All parcels of MIST\_ROI are by definition fully lateralized and hence have a bilaterality score of 0. (Bottom row) Internal homogeneity of parcels across MIST resolutions. Annotated parcels are highlighted in orange. Hover over individual data points to see additional information. The online version of this figure is interactive.

The parcel names included in this release are based on a systematic naming system (outlined below) to ensure consistency.

Naming template:

{hemisphere}\_{NAME}\_{TYPE}\_{position}

Naming example:

{right}\_{MIDDLE\_TEMPORAL}\_{GYRUS}\_{posterior}

All fields except the {NAME} field are optional and only used where they add information to the name.

- **Hemisphere** (lowercase). Only used in fully lateralized parcels. There it describes the brain hemisphere the parcel is located in. Values are
  - left
  - right

Overlap with root parcel at resolution MIST\_7

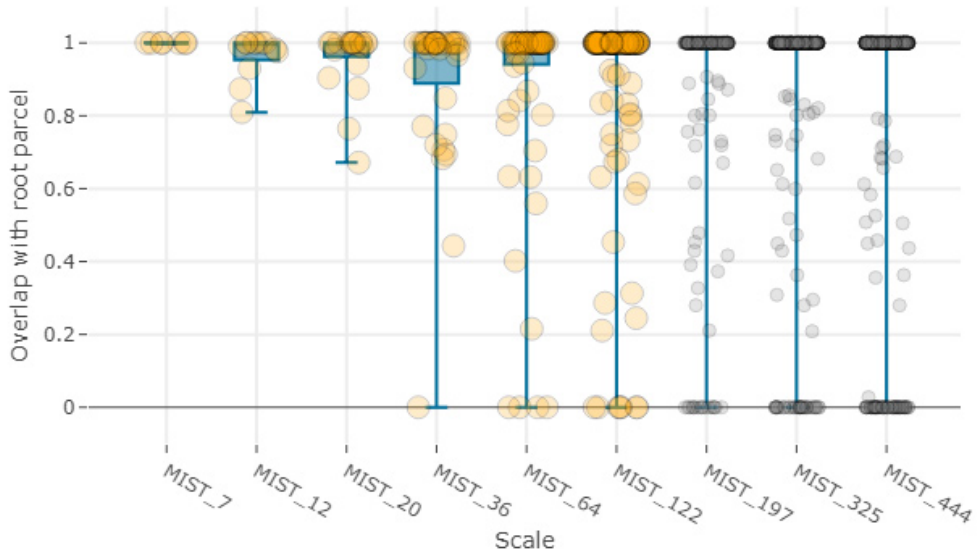


**Figure 4. Overlap with root parcels in the pseudo-hierarchy.** The overlap with the corresponding pseudo-hierarchical root-parcel at MIST\_7 is shown for parcels across resolutions. Overlap is represented in percent overlap of total parcel size. Higher values indicate an assignment more in line with the data derived pseudo-hierarchy. Annotated parcels are highlighted in orange. The online version of this figure is interactive.

- **Name** (uppercase). The name of the parcel.
- **Type** (uppercase). Where applicable describes the type of structure or system the parcel encompasses. Values are:
  - NETWORK
  - GYRUS
  - SULCUS
  - LOBE
  - CORTEX
  - POLE
- **Position** (lowercase). Mostly used for parcels at higher resolutions that are best described by their relative position within larger networks. Values are:
  - anterior / posterior
  - dorsal / ventral
  - lateral / medial

and combinations of these (e.g. anteromedial). The position information can be capitalized as part of the name when the area is commonly known by that name (e.g. Anterior Cingulate Cortex)

For each parcel name we also provide an abbreviated parcel label designed to take up less space while still being informative. The convention for labels follows that of names but uses different upper- and lowercase rules and values:

Label template:

{HEMISPHERE}\_{NAME}{type}\_{position}

Label example:

{R}\_{MT}{gyr}\_{p}

- **Hemisphere** (Uppercase). Unlike the name {hemisphere} field, this is uppercase to avoid confusion with lowercase 'L' characters in some typesets. Only used in fully lateralized parcels. There it describes the brain hemisphere the parcel is located in. Values are
  - L for left
  - R for right

- **Name** (uppercase). The abbreviated name of the parcel. Abbreviating the parcel name is done in a way that retains some distinguishing properties but is as short as possible.

- **Type** (lowercase). Unlike the parcel name {Type} field, this is lowercase to provide a visual distinction from the abbreviated parcel name. Values are:

- net for NETWORK
- gyr for GYRUS
- sul for SULCUS
- lob for LOBE

- cor for CORTEX
  - pol for POLE
  - **Position** (lowercase). Abbreviated version of the position field in the parcel name. Values are:
    - a / p for anterior / posterior
    - d / v for dorsal / ventral
    - l / m for lateral / medial
- and combinations of these (e.g. am for anteromedial).

**Suggested use, limitations and planned improvement of parcel names.** It is important to note that the parcel names are intended to help navigate the parcellations by giving the reader a quick idea where in the brain a parcel is situated. They are not intended for precise delineation of a particular anatomical region or functional pathway. While the parcels names provided with this release are unique, they are also not intended as unique descriptors of individual parcels. We suggest that individual parcels are referred to by their integer ID and parcellation resolution. For example, the parcel 6 of the parcellation resolution 64 should be referred to as 6@MIST\_64.

**Parcel properties.** Apart from individual labels we provide a set of quantitative properties for each parcel.

- **Center of Mass.** We report the center of mass of the parcel in MNI coordinates. Note that the center of mass may lie outside the parcel for bilateral parcels.
- **Size.** This represents the volume of the parcel in voxels. The MIST parcellation is released at a resolution of 3mm isotropic voxels.
- **Laterality.** Our laterality index represents the difference in left and right hemispheric parcel volume as a proportion of the total parcel volume. A parcel with 50% more left than right volume would have a laterality index of 0.5. A perfectly bilateral parcel would have a laterality index of 0.
- **Symmetry.** Our symmetry index represents the dice coefficient between the left and right hemispheric component of a parcel. A fully symmetric parcel would have a symmetry index of 1. A non-symmetric parcel would have a symmetry index of 0.
- **Neighbours.** Parcels with touching voxels in the same resolution are considered neighbours. We report their parcel IDs.
- **Parent.** The parcel ID of the parcel at resolution R-1 with maximal overlap.
- **Parent Overlap.** The proportion of the parcel that overlaps with the parent parcel.

### Quality of hierarchical decomposition

We assessed the accuracy of the hierarchical decomposition of parcels across multiple resolutions. We generated the hierarchy by assigning each parcel to the parcel of the next lower resolution it has the highest overlap with (see Methods for details). A good hierarchical decomposition would result in parcels that

decompose into fully enclosed subparcels. We therefore tested the percent overlap of parcels with their parent parcels across the resolutions. [Our interactive web viewer](#) shows an overview of parcel overlap across resolutions. At every resolution, most parcels have a very high degree of overlap with their parent parcel. Parcels with lower parent overlap are predominantly located along the interface of parietal and occipital lobe and in the lateral prefrontal cortex. The parieto-occipital interface is also a transition area between two large scale functional networks at lower resolution and parcels along this interface could shift across resolutions along the stability gradient of this transition zone. The weighted average of parent overlap across resolutions is very high at 95%, indicating a generally excellent alignment of sub parcels with their parent parcel.

We finally looked at the entire hierarchical decomposition tree to find the overlap of parcels with the root parcel of their decomposition tree. The root parcels are the parcels in the MIST\_7 parcellation for which decomposition across resolutions is tracked independently. While each parcel is assigned to the parcel of the next lower resolution it has the maximal overlap with, incremental non-complete overlaps can accumulate to a point where a parcel no longer has any overlap with the root parcel it is assigned to by our pseudo-hierarchy. Out of 1227 parcels across all nine resolutions (not including MIST\_ROI) we identified 116 parcels that didn't overlap with the root parcel of their hierarchical decomposition tree. Across the MIST resolutions we found parcels with no root overlap in MIST\_36: 1 parcel (3%), MIST\_64: 4 parcels (6%), MIST\_122: 7 parcels (6%), MIST\_197: 16 parcels (8%), MIST\_325: 33 (10%), MIST\_444: 55 parcels (12%). None of these parcels had root-parcels located in the somatomotor, visual or cerebellar networks of MIST\_7. [Figure 4](#) provides an overview of the root-parcel overlap across scales. While it is unclear what factors may cause the gradual shifts of these identified parcels it is important to note that most parcels have high degrees of overlap with both their immediate parent parcels as well as their root-parcels. The MIST pseudo-hierarchy thus captures meaningful cross-resolution relationships between parcels.

### Comparison with existing atlases

The functional connectivity literature is full of brain parcellations based on different methodologies, modalities, and datasets. It is therefore reasonable to ask, what this parcellation can offer the field that isn't already available. In our view, the main contribution of the MIST atlas is the fact that it provides hierarchically linked, and labeled multi-resolution parcellations of the whole brain across the spatial resolutions commonly investigated in the field. In this section we briefly discuss how the MIST parcellation compares to existing parcellations of comparable scope and methodology.

### Multi-resolution parcellations

To our knowledge, there are only three other functional connectivity based multi-resolution parcellations available in the literature: those by Craddock and colleagues<sup>7</sup> and by Shen and colleagues<sup>12</sup> both use approaches building on spectral clustering to derive volumetric, whole brain parcellations. Recent work by Schaefer and colleagues<sup>14</sup> uses the similarity of functional

connectivity in addition to local functional connectivity gradients to define brain parcels on the neo-cortical surface. All three of these multi-resolution parcellations have in common that they aim to provide very homogeneous functional areas at high spatial granularity that can be used as nodes in functional connectivity analyses. This leads to two important differences to the MIST atlas presented here. First, they either directly<sup>7,14</sup> or indirectly<sup>12</sup> force parcels to be spatially contiguous and, with the exception of the Craddock parcellation, lateralized to one hemisphere. Second, they provide parcellations at relatively high resolutions of 100, 200, and 300 parcels in the case of the Shen parcellation, 400 to 1000 parcels in increments of 200 in the case of the Schaefer parcellation, and 50 to 1000 parcels in increments of 50 in the case of the Craddock parcellation.

The objective of the MIST parcellation is related, but conceptually different as it aims to provide a multi-resolution decomposition of the brain beginning with large, spatially non-contiguous networks and ending with functional areas, the spatial resolution that the aforementioned parcellations aim to characterize. This is also reflected in the fact that no spatial constraint is imposed on the parcels of the MIST parcellation (with the exception of the MIST\_ROI parcellation) which are markedly bilateral and non-contiguous up to the highest resolutions. Finally, we have relied on a data-driven method to automatically select the most descriptive resolutions of brain parcellations rather than selecting them at arbitrary intervals.

### Yeo parcellation

Among the wealth of functional brain parcellations available at a single resolution, the works by Yeo<sup>3</sup> and Glasser<sup>6</sup> stand out due to their methodological rigor and the extent of their use in the field (more than 2500 and 720 citations to date respectively). They also stand at opposite ends of the spatial resolution spectrum covered by the MIST parcellation. Their Yeo parcellations represent canonical functional connectivity networks while the Glasser parcellation represents small areas bounded by multi-modal agreement of boundaries.

Yeo and colleagues provide a partition of the cortical surface into large, distributed functional networks at spatial resolutions of 7 and 17 parcels that is based on the similarity of the seed based functional connectivity at 18700 surface vertices. In particular the 7 network parcellation is often considered a parcellation of reference for the canonical resting state connectivity networks that are reliably differentiable, and has informed the labeling of the MIST parcellation at low resolutions. While the Yeo parcellation is generated entirely on the cortical surface, the authors provide a projection into volumetric MNI space that we use to compare it with MIST parcellations of comparable spatial resolution: we compare the 7 Yeo networks to the MIST\_7 parcellation, and the 17 Yeo networks to the MIST20 parcellation. Since the MIST parcellations cover the cerebellum and subcortical areas while the Yeo parcellations do not, we exclude those regions from the comparison and consider only regions in the intersection of the MIST brainmask and the non-zero voxels of the volumetric Yeo parcellation (1 region was removed

from the MIST\_7 parcellation, and 4 regions were removed from the MIST\_20 parcellation).

We compare the parcellations in two ways: First, we determine the spatial overlap of networks by computing the maximal dice coefficient of each MIST network with the corresponding Yeo parcellation. Second, we detect and highlight the border regions between networks in each parcellation in order to qualitatively compare their spatial location.

The average dice coefficient of MIST\_7 networks with Yeo\_7 networks is 68%, with some regional variation (see [Figure 5](#)). The MIST\_7 visual network has a high dice coefficient of 88% with the Yeo\_7 visual network, while the MIST\_7 network comprising the ventral attention and salience network has a lower dice coefficient of 49% with the corresponding Yeo\_7 network (see [Table 2](#) for a complete overview). [Figure 5](#) (left side) gives a spatial representation of the parcel overlap. MIST\_7 visual, somatomotor, default mode and mesolimbic networks show a high degree of spatial overlap with Yeo\_7 parcels, whereas the fronto-parietal and the aforementioned ventral attention network show lower overlap. This is also reflected in the spatial alignment of network borders between the MIST\_7 and Yeo\_7 parcellations ([Figure 5](#), right side). Borders of the visual, somatomotor, limbic and default mode networks of the MIST\_7 parcellation are closely aligned while the detected boundaries in the Yeo\_7 parcellation. By contrast, the frontoparietal and ventral attention network of the MIST\_7 parcellation are intersected by estimated network boundaries of the Yeo\_7 parcellation.

The average dice coefficient of MIST\_20 networks with Yeo\_17 networks is 55%, with considerable regional variation. The lateral and medial visual networks of the MIST\_20 parcellation spatially overlap well with the corresponding Yeo\_17 networks (visual A and visual B) by 85% and 81% respectively. On the other hand, the medial and lateral ventral attention networks of the MIST\_20 parcellation both have dice coefficients with the Yeo\_17 salience and ventral attention network of 33% and 38% respectively (see [Table 3](#) for a full overview).

Several MIST\_20 networks are situated inside larger Yeo\_17 networks. The ventral somatomotor network of MIST\_20 is 82% inside the Yeo\_17 Somatomotor B network, yet has a dice coefficient of only 0.38 with this network. This is because the Yeo\_17 Somatomotor B network extends ventrally beyond the somatomotor strip and includes a portion of the superior temporal lobe that is part of the auditory network in the MIST\_20 parcellation. The MIST\_20 auditory network is 60% inside the Yeo\_7 Somatomotor B network. Other cases are less clear. The MIST\_20 perigenual ACC and VMPFC network is 72% inside the larger Yeo\_17 Default mode network A, but the three MIST\_20 DMN sub-networks (anterior, posteromedial, and lateral DMN) do not align closely with the three Yeo\_17 DMN sub-networks (Default Mode network A–C) (see [Table 3](#)). [Figure 5](#) (B: right column) gives some indication for the reason behind this: the border of the MIST\_20 posteromedial DMN sub-network extends further into the precuneus than that of the Yeo\_17 Default

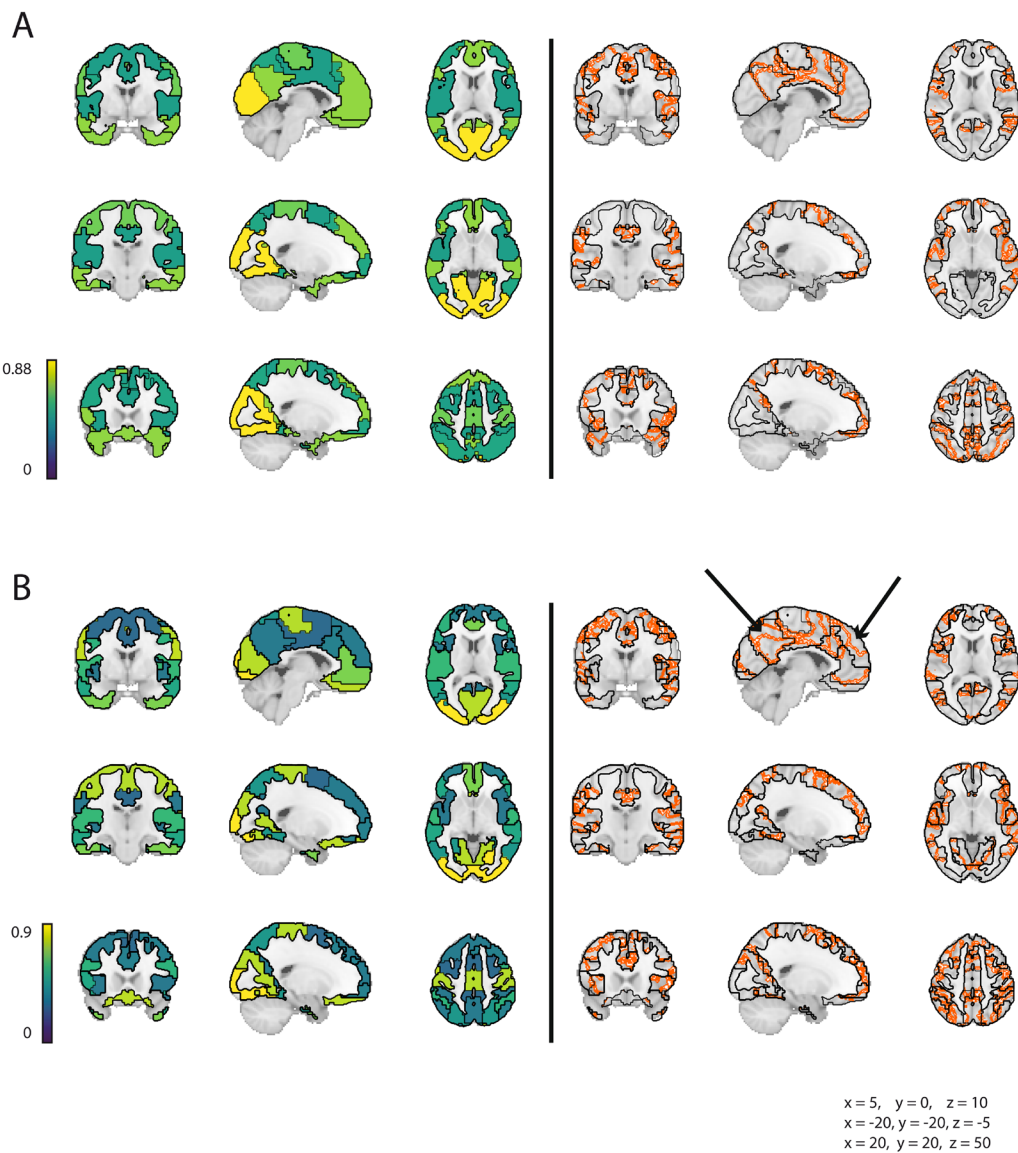


**Figure 5. Similarity of MIST and Yeo parcellation.** Left column: MIST networks are color coded by their spatial overlap (dice) on corresponding Yeo networks<sup>5</sup>. Right column: the borders of the MIST networks (black line) are overlaid over the transition zones between Yeo networks to illustrate local differences in network outlines (black arrows). **A:** MIST\_7 networks and Yeo\_7 networks **B:** MIST\_20 networks and Yeo\_17 networks.

Mode A network. Similarly, the border of the MIST\_20 anterior DMN sub-network extends further ventrally and caudally along the medial surface than that of the Yeo\_17 Default Mode B network (see black arrows).

Overall, visual, motor and limbic networks of the MIST\_20 parcellation are well aligned with their Yeo\_17 counterparts. The agreement of network boundaries is lower for the sub-networks of the DMN, the fronto-parietal and the ventral- and dorsal attention networks. The lower agreement between MIST\_20 and Yeo\_17 compared with the higher alignment of the MIST\_7 and Yeo\_7 parcellation are due to differences in the way large networks split into sub-sections at the higher spatial resolution (such as in the case of the Yeo\_17 Somatomotor B

network that includes temporal areas but otherwise aligns very closely to the MIST\_20 ventral somatomotor network). Other differences are due to differences in alignment of network boundaries that may reflect instabilities of functional network membership in these areas, differences of methodology, or factors due to higher inter-subject variability of functional connectivity in these areas that influence the group level parcellations<sup>33</sup>. Investigating these factors further goes beyond the scope of this work.

#### Glasser parcellation

Glasser and colleagues provide a widely used parcellation of the neo-cortical surface into homogeneous functional areas that is based on a combination of imaging modalities: resting state fMRI

connectivity, task based fMRI activation, local myelination, and cortical thickness. The boundaries of functional areas in this parcellation are defined by overlapping gradient maxima in at least two of these modalities with additional weight given to gradients with contralateral homologues. The Glasser parcellation defines 360 functional areas, 180 per hemisphere. Like the Yeo parcellation, it is generated entirely on the cortical surface. While a projection to volumetric MNI space exists, the projection covers a very narrow band along the cortical ribbon and only covering only 51% of the volumetric parcels of the MIST\_444 parcellation (excluding subcortical areas and the cerebellum, 387 parcels remain). A related difference that of size of the parcels when compared in their volumetric representations. The Glasser\_360 parcels naturally follow closely the cortical surface, spanning different gyri. By contrast, the volumetric MIST\_444 parcels are more localized in space and cover smaller areas on the cortical surface. As a result, when applying the consensus mask between both parcellations, the Glasser\_360 parcels are on average more than twice as large.

Due to these differences, we attempted only a cursory comparison between the MIST\_444 parcellation and the Glasser\_360 parcellation. As the dice coefficient is not well suited to reflect alignment between parcels of very different sizes, we instead directly measured the maximal overlap of the MIST\_444 parcellation with parcels in the Glasser\_360 parcellation (i.e. we measured which percentage of the MIST\_444 parcel is within

the bounds of a Glasser\_360 parcel of maximal overlap). The average overlap of MIST\_444 parcels on Glasser\_360 parcels is 50%, with a wide variability of values from 7% to 100% (the median is 47%). [Figure 6](#) shows a projection of computed overlap of MIST\_444 parcels onto the surface, revealing areas of higher parcel overlap within primary visual cortex, middle temporal gyrus, and sections of the dorsal ventromedial prefrontal cortex. Areas of low alignment are within the somatomotor strip, the precuneus and anterior cingulate cortex.

It is worth pointing out, that the Glasser parcellation is methodologically very different from the MIST parcellation, in terms of spatial scope (cortical surface vs whole-brain volume), in terms of underlying data (high-resolution data of multiple modalities vs functional data of average resolution), and in terms of procedure (manually guided automatic parcellation based on local transition gradients vs unsupervised parcellation based on global similarity of connectivity). Nevertheless, both the Glasser\_360 and the MIST\_444 parcellations aim to provide a description of functional areas that can be assumed to be internally functionally homogeneous for the purposes of dimensionality reduction and node definition. Perhaps a more relevant metric is therefore the question of internal homogeneity of parcels. Here both parcellations perform very similarly with an average internal homogeneity of 0.5 for the MIST\_444 parcellation and of 0.46 for the Glasser\_360 parcellation (see [Figure 7](#)).

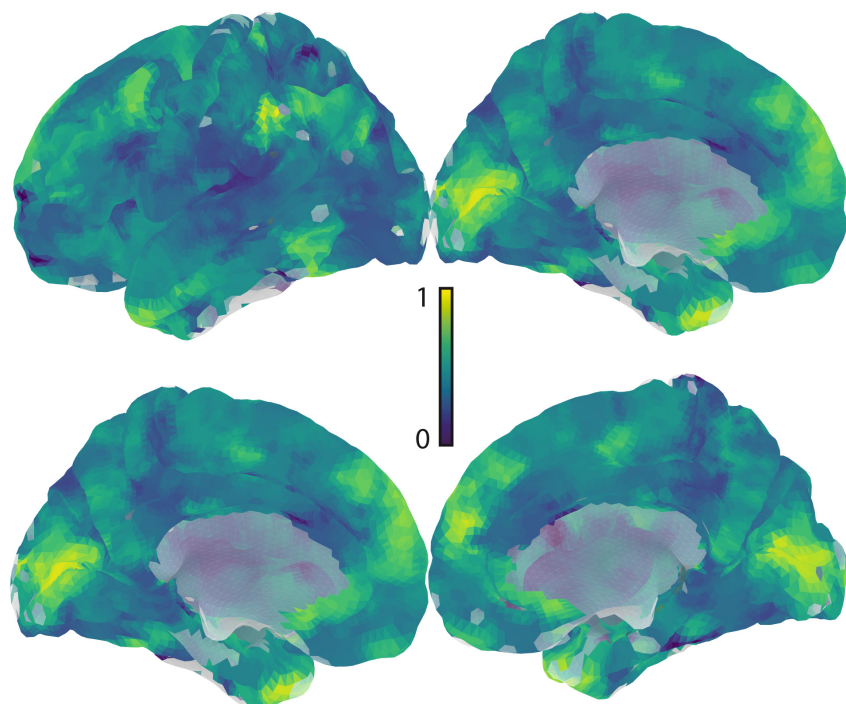


**Figure 6. Similarity of MIST and Glasser parcellation.** The MIST\_444 areas are projected onto the cortical surface and color coded by their spatial overlap (percent overlap) on the corresponding Glasser<sup>8</sup> areas. Note that this comparison has limited practical value since the spatial extent of MIST and Glasser areas is very different.

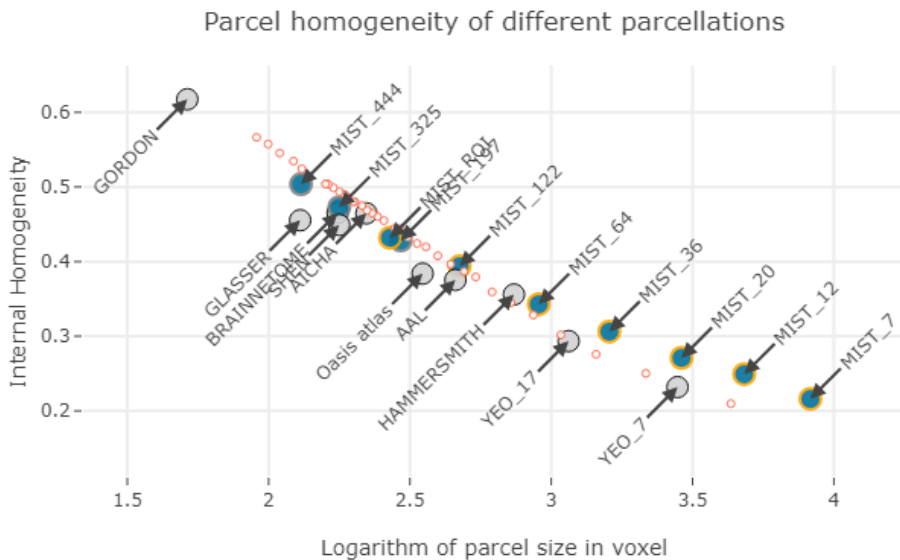


**Figure 7. Comparison with other parcellations.** The standard deviation (SD) of homogeneity estimates across individuals in the HNU1 data set is shown as a function of the common logarithm of the average parcel size. Lower scores reflect lower variability in homogeneity estimates between individuals. Annotated parcellations are highlighted with an outline in orange. Random parcellations are shown as smaller white circles with a red outline for reference. The online version of this figure is interactive.

### Other parcellations

To quantitatively compare the quality of our parcellations to other, existing functional connectivity parcellations we estimated the within parcel functional homogeneity, a common quality metric in the literature<sup>11,34</sup>. A good functional brain parcel is expected to encompass voxels with reasonably similar functional activity. Here we estimate the functional homogeneity of a parcel as the average functional connectivity between its voxels. All other things being equal, smaller parcels will have higher internal homogeneity than larger ones, particularly when they are spatially contiguous. We therefore compute the global homogeneity of a parcellation as the size-weighted average of its individual parcels.

We compare our parcellations to a number of published brain parcellations in the literature (see Table 1). Parcellations that were generated on surface data were back-projected into MNI volumetric space. As a consequence, brain coverage differs between parcellations with some covering only the cortical ribbon while others also providing parcellations of subcortical regions and the cerebellum. A parcellation with only cortical coverage will on average have smaller parcels than a full brain parcellation of the same resolution. To account for parcel-size dependent differences in homogeneity, we therefore opted to compare parcellations based on the average size of their parcels (in voxels). Lastly, we included a random multi-resolution parcellation generated by Craddock and colleagues<sup>7</sup>. These random parcels are entirely driven by spatial proximity and since they have been reported to perform about as well as functionally defined parcels of similar size, we included them in this analysis as a point of comparison. All parcellations were resampled to 3mm isotropic voxels to allow for a direct comparison.

To conduct the quality assessments we used the openly available HNU1 dataset from the Consortium for Reliability and Reproducibility<sup>35</sup> that provides 10 repeat session of fMRI data acquired over the course of a month for 30 individuals. This dataset allows us to average our quality metrics across sessions per individual, giving a more stable estimate. In addition none of the compared brain parcellations has been generated on this data, providing an unbiased estimate of performance on other datasets. Data were preprocessed and quality controlled according to the protocol described above. 27 individuals (15 female, mean age 24.5 years, SD 2.4) were included in the analysis.

Figure 7 shows the global homogeneity of parcels over the logarithm of the average parcel size. The relationship between homogeneity and parcel size is clearly visible in the exponential decline of homogeneity with parcel size. Our multi-resolution parcellations compare well with other parcellations of similar parcel size, particularly at lower resolutions. A second question is how consistent the estimated homogeneity scores are across individuals. High consistency of homogeneity indicates that a parcellation generalizes well across individuals whereas a low consistency indicates a very case-dependent fit of the parcellation to the individual functional architecture. Figure 8 shows the standard deviation of homogeneity estimates across subjects as a function of the logarithm of average parcel size. Larger parcels show lower standard deviation of homogeneity across individuals. Again, our parcels fall well within the range of cross-subject consistency of other data driven atlases with comparable resolutions.

The random Craddock parcellations we included as a point of comparison show homogeneity values with a strikingly

**Table 1.** Published brain parcellations that were compared to the MIST parcellation.

Name	Coverage	Resolution	Sample	Description
OasisTRT <sup>36</sup>	Whole brain	94 (mean size: 350 voxels)	20	Consensus partition generated by joint label fusion <sup>37</sup> based on 20 manually annotated anatomical brain scans.
Yeo7 <sup>3</sup>	Cortical surface	7 (mean size: 2797 voxels)	1000	Clustering of functional connectivity profiles at 1175 ROI locations across the cortical surface. The 7 and 17 networks solutions were chosen as a compromise between stability and resolution range.
Yeo17 <sup>3</sup>	Cortical surface	17 (mean size: 1152 voxels)	1000	
AAL2 <sup>38</sup>	Whole brain	120 (mean size: 458 voxels)	1	Manual delineation along anatomical landmarks (sulci) in a single brain. Updated version of the original AAL parcellation <sup>39</sup> .
Aicha <sup>40</sup>	Cortical and subcortical (no cerebellum)	192 (mean size: 222 voxels)	281	Functional connectivity based parcellation using k-means clustering and grouping of parcels by functional homotopy based on inter-hemispheric connectivity.
Brainnetome <sup>41</sup>	Whole brain	273 (mean size: 175 voxels)	40	Functional and anatomical connectivity based subdivision of anatomically defined brain regions based on Desikan <sup>2</sup> using spectral clustering.
Hammersmith <sup>42</sup>	Whole brain	83 (mean size: 734 voxels)	30	Consensus parcellation of 30 manually annotated anatomical brain scans.
Shen <sup>12</sup>	Whole brain	268 (mean size: 178 voxels)	79	Functional connectivity based parcellations using spectral clustering that emphasizes parcel homogeneity.
Gordon <sup>11</sup>	Cortical surface	333 (mean size: 52 voxels)	120	Cortical parcellation based on functional connectivity gradients. Parcels are grown and merged with respect to connectivity boundaries.
Glasser <sup>6</sup>	Cortical surface	180 (mean size: 129 voxels)	210	Semi-automatic segmentation along cortical gradients of architectural, functional, connectivity, and topographic modalities as well as expert ratings.
Craddock <sup>7</sup>	Whole brain	Multi-Resolution	41	Random multi-resolution parcellation based on spectral clustering of spatial proximity.

**Table 2.** Spatial overlap of MIST\_7 and Yeo\_7 networks.

MIST_7 network	Yeo_7 network	OVLP	DICE
Visual network	Visual	0.96	0.88
Somatomotor network	Somatomotor	0.88	0.69
<b>No maximal overlap parcel</b>	Ventral Attention		
Ventral attention and salience network	Dorsal Attention	0.37	0.49
Mesolimbic network	Limbic	0.66	0.73
Frontoparietal and visual downstream	Fronto-parietal	0.41	0.52
Default Mode network	Default mode	0.81	0.74

logarithmic dependence on the average parcel size. At lower resolutions (i.e. larger parcel sizes), the random parcellations have lower internal homogeneity values than connectivity derived parcellations of similar resolution. Around a resolution of 120 parcels (i.e. parcels of around 473 3mm voxels) the internal homogeneity values of the random Craddock parcellations start to exceed those of connectivity driven parcellations. This

change in relative performance is probably due to the inability of a random parcellation to capture distributed, large scale functional networks at lower resolutions whereas at higher resolutions, a bias towards spatially contiguous parcels of similar size seems to be advantageous. The consistency of internal homogeneity estimates of the random Craddock parcels also shows a dependence on spatial resolution and is overall lower

**Table 3. Spatial overlap of MIST\_20 and Yeo\_17 networks.** Names for the Yeo\_17 networks are taken from Yeo *et al.*, 2015<sup>43</sup>.

MIST_20	Yeo_17 network	OVLP	DICE
lateral visual network	Visual A	0.90	0.85
medial visual network	Visual B	0.80	0.81
dorsal somatomotor network	SomMot A	0.80	0.82
ventral somatomotor network	SomMot B	0.82	0.38
auditory network		0.60	0.58
ventral and dorsal visual stream	Dorsal Att A	0.48	0.59
<b>No maximal overlap parcel</b>	Dorsal Att B		
medial ventral attention network	Sal/Vent Att A	0.31	0.33
lateral ventral attention network	Sal/Vent Att A	0.36	0.38
<b>No maximal overlap parcel</b>	Sal/Vent Att B		
ITG and temporal pole	Limbic B	0.72	0.82
orbitofrontal cortex	Limbic A	0.81	0.70
<b>No maximal overlap parcel</b>	Control C		
Frontoparietal and task control network	Control A	0.58	0.52
Frontoparietal network	Control B	0.39	0.42
<b>No maximal overlap parcel</b>	TempPar		
<b>No maximal overlap parcel</b>	Default Mode C		
perigenual ACC and VMPFC	Default Mode A	0.72	0.35
posteromedial DMN		0.38	0.46
anterior DMN	Default Mode B	0.38	0.35
lateral DMN		0.54	0.48

### Consistency of homogeneity estimates across subjects

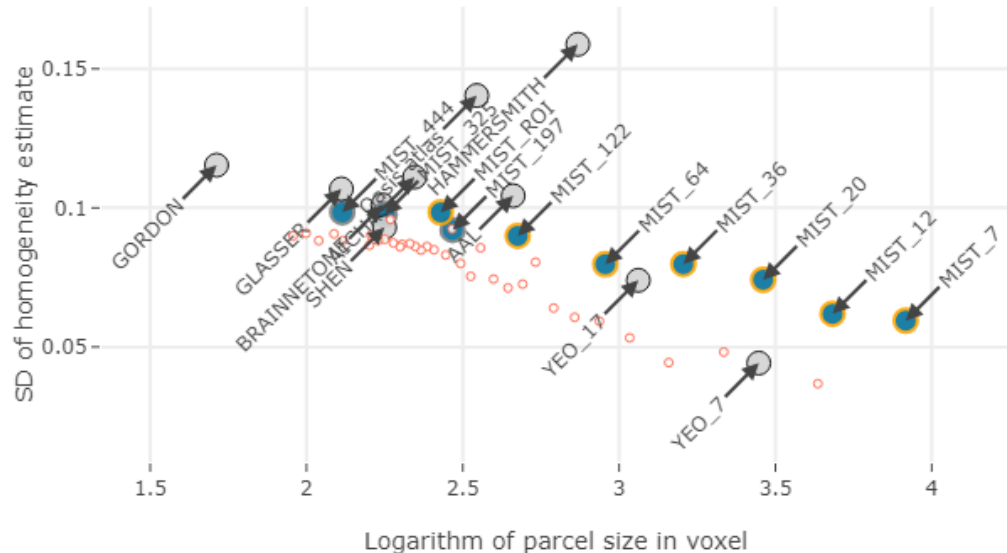


**Figure 8. Consistency of homogeneity estimates as a function of parcel size.** Global parcel homogeneity of MIST parcellations and commonly used other brain parcellations of comparable size and focus. Homogeneity estimates are plotted over the common logarithm of the average parcel size. Higher scores reflect more homogeneous parcels. Annotated parcellations are highlighted with an outline in orange. Random parcellations are shown as smaller white circles with a red outline for reference. The online version of this figure is interactive.

than that of the data driven parcellations. While the random Craddock parcellations were found to perform about as well as similar connectivity derived parcellations in previous work<sup>7</sup>, the strong performance at high resolutions observed here warrants further investigation.

### Generalizability of parcellation

A good functional brain parcellation can be expected to provide parcels that are not only reasonably homogeneous but also reasonably independent of the dataset used to generate them. We address this question by testing the reproducibility of our parcellation using two approaches: First, we randomly split our original dataset in half, regenerate the full set of parcellations on

each subset and compare the alignment with the original MIST parcellation. Second, we repeat this process on the publicly available Genome Superstruct Project (GSP)<sup>44</sup>, a new dataset with comparable acquisition parameters but a considerably larger sample size. The GSP data were preprocessed in the same way as our original dataset and after quality control contained 1562 individuals with two scan sessions each. We regenerated the MIST parcellation on each session separately and compared the alignment with the original MIST parcellation.

**Figure 9** shows the dice coefficient between parcels of the MIST parcellations those in each of the split-half replication parcellations. Replication performance in both split-half subsam-

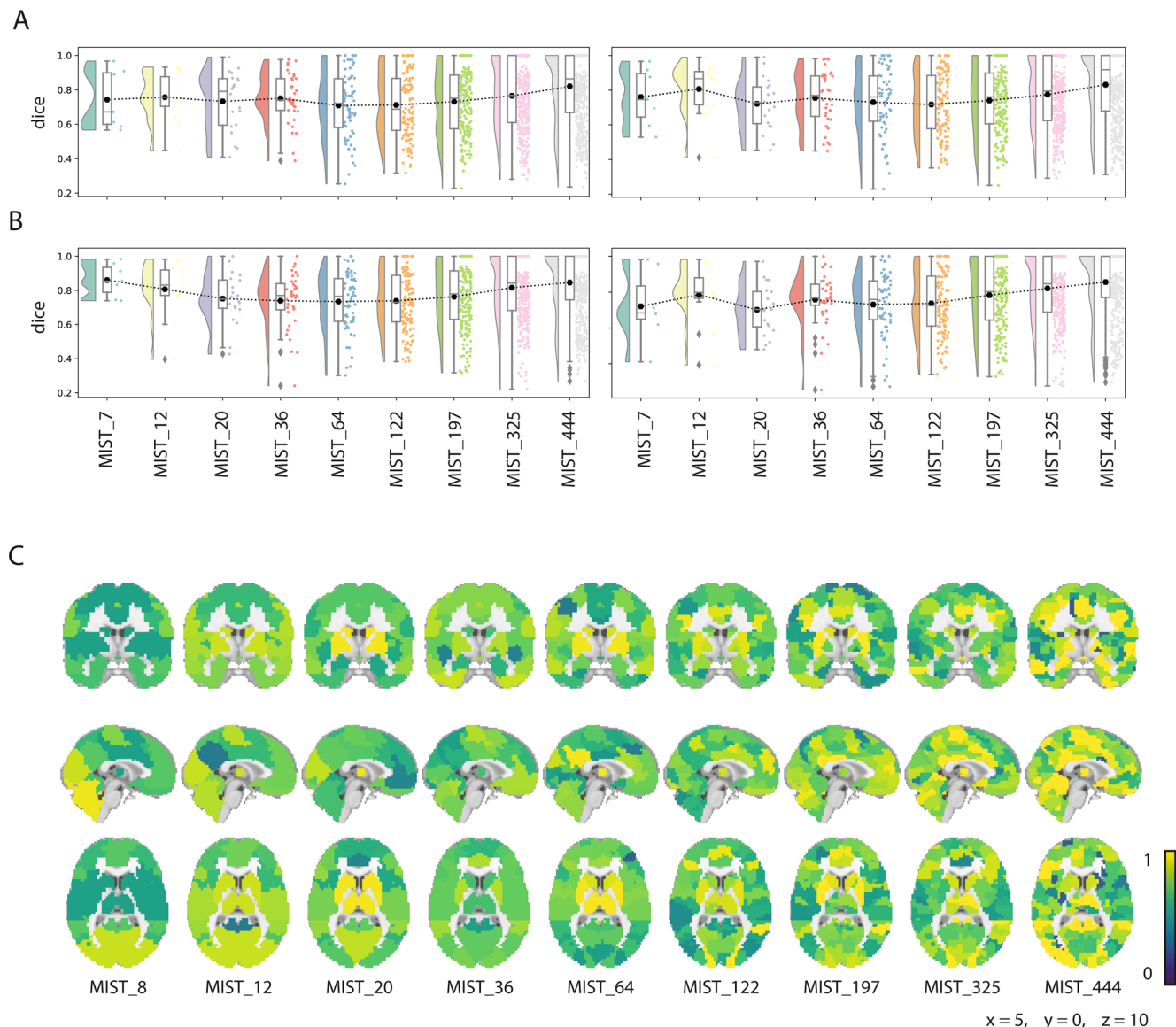


**Figure 9. Reproducibility of the MIST parcellations.** **A:** The spatial reproducibility of MIST parcels (dice with original parcellation) is shown within the first (left) and second (right) split-half replication sample of the original Cambridge dataset. **B:** The spatial reproducibility of MIST parcels (dice with original parcellation) is shown within the first (left) and second (right) session of the GSP Cambridge dataset. **C:** The original MIST parcels are color coded based on their average reproducibility (dice with original parcel) across all replication datasets (both split-half samples and both GSP sessions).

ples is very similar. The average dice between the original and replication parcellation is 0.75 across all spatial resolutions and both split-half subsamples. There is some variability of the replication performance across the spatial resolutions with higher spatial resolutions showing higher average dice coefficients (dashed black lines in Figure 9). There is considerable variability among the dice scores for different parcels. At lower spatial resolutions, we observe higher dice coefficients in primary sensory areas such as the visual, somatomotor, and auditory network and the cerebellum and lower dice coefficients in more associative networks. This mirrors the results of our comparison between the MIST parcellation and the Yeo parcellation (see the section on Comparison with existing atlases) and is very consistent between the two split-half replication samples. At higher spatial resolutions, areas of high and low dice coefficients become more distributed and include more frontal areas such as the anterior cingulate and VMPFC.

Our replication test in the much larger GSP dataset reveals very similar findings. The average dice coefficient across both GSP sessions and all MIST parcellations is 0.77. Figure 9 shows the distribution of parcel-level dice coefficients in the GSP and exhibits a similar increase of the average dice coefficient with spatial resolution. Consistent with our findings in the split-half replication, we find a pattern of higher reproducibility in visual, and somatomotor networks and the cerebellum, that is very consistent between the two GSP sessions and becomes more distributed at higher spatial resolutions.

These values, while not perfect, are consistent with what has been reported in the literature [e.g. 14] and may be more reflective of the general limitations of group parcellations to capture individual variability<sup>45,46</sup>, rather than the quality of the specific parcellation.

### Predictive performance

Another way to look at the generalizability of the MIST parcellation is to test its performance in real world applications. One of the most common applications for a functional brain parcellation is to define nodes in a functional connectivity analysis. A reasonable assumption is then that better parcels will lead to more generalizable models of functional connectivity. Dadi and colleagues have tested the impact of different brain parcellation methods (and other processing parameters) on the prediction of clinical traits based on the functional connectomes estimated from these parcellations<sup>47,48</sup>. Prediction performance was compared across three pre-generated atlases (the Harvard-Oxford Atlas, the AAL atlas, and the MIST\_64 parcellation) and a set of custom parcellations derived directly from the data using a range of methods (ICA, dictionary learning, K-means clustering, and Hierarchical clustering using Ward's criterion). The authors found that across several prediction problems based on several datasets (including Schizophrenia on the COBRE dataset, Alzheimer's disease based on the ADNI dataset, and Autism based on the ABIDE dataset), the MIST\_64 parcellation performed consistently well, above the other pre-generated atlases and “almost as well as the best regions-extraction method applied to the rest-fMRI data of interest”.

### Conclusion

With the MIST parcellation, we have generated and publicly released a multi-resolution decomposition of large functional networks into localized functional areas. With the parcellation we provide annotations for parcels at all resolutions and a data-derived decomposition tree that situates individual parcels along a cross-resolution hierarchy that have no published equivalent in the functional parcellation literature. We show that the MIST parcellations at individual resolutions fit well into the existing literature of brain parcellations in terms of spatial alignment, reproducibility, internal homogeneity, and generalizability. The multiresolution nature of the MIST parcellation will make it a valuable new resource for connectivity researchers.

### Data availability

The MIST parcellation is available from figshare (<https://doi.org/10.6084/m9.figshare.5633638.v1><sup>49</sup>). The code used to perform the analyses described in this work can be found at: [https://github.com/suruchs/MIST\\_atlas](https://github.com/suruchs/MIST_atlas). The code used to generate the interactive atlas viewer can be found at: [https://github.com/SIMEXP/multi-scale\\_dashboard](https://github.com/SIMEXP/multi-scale_dashboard). All MIST resolutions as well as MIST\_ROI and the functional atoms used in the BASC process (MIST\_ATOM) to generate the MIST parcellation are available in nifti format. The release contains the following folders:

- **Parcellations**

Contains the MIST parcellations as nifti files at 3mm isotropic voxels in the ICBM2009b space<sup>50</sup>. Each file contains a 3D volume with voxel integer values corresponding to the roi ID of each parcel at that resolution.

- **Parcel\_Information**

Contains parcel properties, name and label information for each parcel. Files are organized by resolutions and are provided for resolutions 7 through 444 and MIST\_ROI. Resolutions MIST\_197, MIST\_333 and MIST\_444 are not annotated and only contain parcel properties. The files are organized as semicolon delimited tabular data with the following columns:

- *roi*. The roi ID of the parcel
- *label*. The abbreviated name of the parcel when available, otherwise the roi ID.
- *name*. The long-form name of the parcel when available, otherwise the roi ID.
- *size*. The volume of the parcel in 3mm isotropic voxels
- *symmetry*. The dice coefficient of the left- and right-hemispheric portion of the parcel
- *laterality*. The percent volume of the total parcel volume that is in excess in one hemisphere
- *x, z, y*. The center of mass of the parcel in MNI coordinates
- *neighbour*. The list of parcels at the same resolution that have facing edges with the parcel

## - Hierarchy

Contains the data derived hierarchical organization of parcels across resolutions as comma separated tabular data. Due to the nature of the MIST\_ROI parcellation, this folder contains two files:

- *MIST\_PARCEL\_ORDER.csv*. Columns are MIST resolutions from MIST\_7 to MIST\_ATOM, excluding MIST\_ROI. Rows are parcel roi IDs in the corresponding resolutions. The table is meant to be read from right to left. Starting with the roi ID of a MIST\_ATOM parcel, one finds the parent parcel at the next lower resolution in the next left column and so on. As a consequence, only the last column contains unique elements, parcel roi IDs in columns of every lower resolution are repeated as often as necessary for all decompositions.
- *MIST\_PARCEL\_ORDER\_ROI.csv*. Like *MIST\_PARCEL\_ORDER.csv* but only for the labeled resolutions MIST\_7 through MIST\_122, and MIST\_ROI and MIST\_ATOM. Provides information on the decomposition of MIST\_122 into MIST\_ROI.

Data are available under the terms of the [Creative Commons Zero “No rights reserved” data waiver](#) (CC0 1.0 Public domain dedication).

## Grant information

This work was supported by grants from Brain Canada (JA, JSA), Brain Canada (SU, CM), Azrieli foundation (SU), Natural Sciences and Engineering Research Council (YB), as well as a salary award by Fonds de Recherche du Québec - Santé (FRQS) and the Courtois foundation to PB.

## Acknowledgments

The computational resources used to perform the data analysis were provided by [Compute Canada](#), and were funded in part by NSERC, FQRNT, and McGill University.

We would like to thank AmanPreet Badhwar, Angela Tam, and Perrine Ferré for their comments and suggestions of parcel names. For their feedback and contributions to writing the manuscript of this publication we want to thank Christian Dansereau, Jake Vogel, Angela Tam, Esther Schott, and AmanPreet Badhwar.

## References

1. Brodmann K: **Vergleichende Lokalisationslehre der Großhirnrinde: in ihren Prinzipien dargestellt auf Grund des Zellenbaues.** Leipzig: Johann Ambrosius Barth; 1909.  
**Reference Source**
2. Desikan RS, Ségonne F, Fischl B, et al.: **An automated labeling system for subdividing the human cerebral cortex on MRI scans into gyral based regions of interest.** *NeuroImage*. 2006; 31(3): 968–80.  
[PubMed Abstract](#) | [Publisher Full Text](#) | [Free Full Text](#)
3. Yeo BT, Krienen FM, Sepulcre J, et al.: **The organization of the human cerebral cortex estimated by intrinsic functional connectivity.** *J Neurophysiol*. 2011; 106(3): 1125–65.  
[PubMed Abstract](#) | [Publisher Full Text](#) | [Free Full Text](#)
4. Power JD, Cohen AL, Nelson SM, et al.: **Functional network organization of the human brain.** *Neuron*. 2011; 72(4): 665–78.  
[PubMed Abstract](#) | [Publisher Full Text](#) | [Free Full Text](#)
5. Hawrylycz M, Miller JA, Menon V, et al.: **Canonical genetic signatures of the adult human brain.** *Nat Neurosci*. 2015; 18(12): 332–44.  
[PubMed Abstract](#) | [Publisher Full Text](#) | [Free Full Text](#)
6. Glasser MF, Coalson TS, Robinson EC, et al.: **A multi-modal parcellation of human cerebral cortex.** *Nature*. 2016; 536(7615): 171–8.  
[PubMed Abstract](#) | [Publisher Full Text](#) | [Free Full Text](#)
7. Craddock RC, James GA, Holtzheimer PE 3rd, et al.: **A whole brain fMRI atlas generated via spatially constrained spectral clustering.** *Hum Brain Mapp*. Wiley Subscription Services, Inc., A Wiley Company; 2012; 33(8): 1914–28.  
[PubMed Abstract](#) | [Publisher Full Text](#) | [Free Full Text](#)
8. Eickhoff SB, Constable RT, Yeo BT: **Topographic organization of the cerebral cortex and brain cartography.** *NeuroImage*. 2018; 170: 332–347.  
[PubMed Abstract](#) | [Publisher Full Text](#) | [Free Full Text](#)
9. Bellec P, Benhajali Y, Carbonell F, et al.: **Impact of the resolution of brain parcels on connectome-wide association studies in fMRI.** *NeuroImage*. 2015; 123: 212–28.  
[PubMed Abstract](#) | [Publisher Full Text](#)
10. Thirion B, Varoquaux G, Dohmatob E, et al.: **Which fMRI clustering gives good brain parcellations?** *Front Neurosci*. 2014; 8: 167.  
[PubMed Abstract](#) | [Publisher Full Text](#) | [Free Full Text](#)
11. Gordon EM, Laumann TO, Adeyemo B, et al.: **Generation and Evaluation of a Cortical Area Parcellation from Resting-State Correlations.** *Cereb Cortex*. 2016; 26(1): 288–303.  
[PubMed Abstract](#) | [Publisher Full Text](#) | [Free Full Text](#)
12. Shen X, Tokoglu F, Papademetris X, et al.: **Groupwise whole-brain parcellation from resting-state fMRI data for network node identification.** *NeuroImage*. 2013; 82: 403–15.  
[PubMed Abstract](#) | [Publisher Full Text](#) | [Free Full Text](#)
13. Van Essen DC, Glasser MF, Dierker DL, et al.: **Parcellations and hemispheric asymmetries of human cerebral cortex analyzed on surface-based atlases.** *Cereb Cortex*. 2012; 22(10): 2241–2262.  
[PubMed Abstract](#) | [Publisher Full Text](#) | [Free Full Text](#)
14. Schaefer A, Kong R, Gordon EM, et al.: **Local-Global Parcellation of the Human Cerebral Cortex from Intrinsic Functional Connectivity MRI.** *Cereb Cortex*. 2018; 28(9): 3095–3114.  
[PubMed Abstract](#) | [Publisher Full Text](#) | [Free Full Text](#)
15. Orban P, Doyon J, Petrides M, et al.: **The Richness of Task-Evoked Hemodynamic Responses Defines a Pseudohierarchy of Functionally Meaningful Brain Networks.** *Cereb Cortex*. 2015; 25(9): 2658–69.  
[PubMed Abstract](#) | [Publisher Full Text](#) | [Free Full Text](#)
16. Meskaldji DE, Vasung L, Romascano D, et al.: **Improved statistical evaluation of group differences in connectomes by screening-filtering strategy with application to study maturation of brain connections between childhood and adolescence.** *NeuroImage*. 2015; 108: 251–64.  
[PubMed Abstract](#) | [Publisher Full Text](#)
17. Badhwar A, Tam A, Dansereau C, et al.: **Resting-state network dysfunction in Alzheimer’s disease: a systematic review and meta-analysis.** *bioRxiv*. 2017; 108282.  
[Publisher Full Text](#)
18. Bellec P, Rosa-Neto P, Lyttelton OC, et al.: **Multi-level bootstrap analysis of stable clusters in resting-state fMRI.** *NeuroImage*. 2010; 51(3): 1126–39.  
[PubMed Abstract](#) | [Publisher Full Text](#)
19. Abraham A, Pedregosa F, Eickenberg M, et al.: **Machine learning for neuroimaging with scikit-learn.** *Front Neuroinform*. 2014; 8: 14.  
[PubMed Abstract](#) | [Publisher Full Text](#) | [Free Full Text](#)
20. Urchs S, Dansereau C, Benhajali Y, et al.: **Group multiscale functional template generated with BASC on the Cambridge sample.** *Figshare*. 2015.  
[Publisher Full Text](#)
21. Liu H, Stufflebeam SM, Sepulcre J, et al.: **Evidence from intrinsic activity that asymmetry of the human brain is controlled by multiple factors.** *Proc Natl Acad Sci U S A*. 2009; 106(48): 20499–503.  
[PubMed Abstract](#) | [Publisher Full Text](#) | [Free Full Text](#)
22. Biswal BB, Mennes M, Zuo XN, et al.: **Toward discovery science of human brain function.** *Proc Natl Acad Sci U S A*. 2010; 107(10): 4734–9.  
[PubMed Abstract](#) | [Publisher Full Text](#) | [Free Full Text](#)

23. Bellec P, Carbonell FM, Perlbarg V, et al.: **A neuroimaging analysis kit for Matlab and Octave.** *Proceedings of the 17th International Conference on Functional Mapping of the Human Brain.* 2011; 2735–46.  
**Reference Source**
24. Eaton JW, Bateman D, Hauberg S, et al.: **GNU Octave version 4.2.0 manual: a high-level interactive language for numerical computations.** 2016.  
**Reference Source**
25. Evans AC, Kamber M, Collins DL, et al.: **An MRI-Based Probabilistic Atlas of Neuroanatomy.** *Magnetic Resonance Scanning and Epilepsy.* Springer, Boston, MA; (NATO ASI Series), 1994; **264:** 263–74.  
**Publisher Full Text**
26. Power JD, Barnes KA, Snyder AZ, et al.: **Spurious but systematic correlations in functional connectivity MRI networks arise from subject motion.** *NeuroImage.* 2012; **59**(3): 2142–54.  
**PubMed Abstract** | **Publisher Full Text** | **Free Full Text**
27. Lund TE, Madsen KH, Sidaros K, et al.: **Non-white noise in fMRI: does modelling have an impact?** *NeuroImage.* 2006; **29**(1): 54–66.  
**PubMed Abstract** | **Publisher Full Text**
28. Giove F, Gili T, Iacovella V, et al.: **Images-based suppression of unwanted global signals in resting-state functional connectivity studies.** *Magn Reson Imaging.* 2009; **27**(8): 1058–64.  
**PubMed Abstract** | **Publisher Full Text**
29. Benhajali Y, Bellec P: **Quality Control and assessment of the NIAK functional MRI preprocessing pipeline.** *figshare.* 2016.  
**Publisher Full Text**
30. Bellec P, Perlbarg V, Jbabdi S, et al.: **Identification of large-scale networks in the brain using fMRI.** *NeuroImage.* 2006; **29**(4): 1231–43.  
**PubMed Abstract** | **Publisher Full Text**
31. Bellec P: **Mining the Hierarchy of Resting-State Brain Networks: Selection of Representative Clusters in a Multiscale Structure.** *Pattern Recognition in Neuroimaging (PRNI), 2013 International Workshop on,* 2013; 54–7.  
**Publisher Full Text**
32. Ad-Dab'bagh Y, Lyttelton O, Muehlboeck JS, et al.: **The CIVET image-processing environment: a fully automated comprehensive pipeline for anatomical neuroimaging research.** *Proceedings of the 12th annual meeting of the organization for human brain mapping.* M. Corbetta. 2006; S45.  
**Reference Source**
33. Mueller S, Wang D, Fox MD, et al.: **Individual variability in functional connectivity architecture of the human brain.** *Neuron.* 2013; **77**(3): 586–595.  
**PubMed Abstract** | **Publisher Full Text** | **Free Full Text**
34. Arslan S, Ktena SI, Makropoulos A, et al.: **Human brain mapping: A systematic comparison of parcellation methods for the human cerebral cortex.** *NeuroImage.* 2018; **170:** 5–30.  
**PubMed Abstract** | **Publisher Full Text**
35. Zuo XN, Anderson JS, Bellec P, et al.: **An open science resource for establishing reliability and reproducibility in functional connectomics.** *Sci Data.* 2014; **1:** 140049.  
**PubMed Abstract** | **Publisher Full Text** | **Free Full Text**
36. Klein A, Tourville J: **101 labeled brain images and a consistent human cortical labeling protocol.** *Front Neurosci.* 2012; **6:** 171.  
**PubMed Abstract** | **Publisher Full Text** | **Free Full Text**
37. Wang H, Suh JW, Das SR, et al.: **Multi-Atlas Segmentation with Joint Label Fusion.** *IEEE Trans Pattern Anal Mach Intell.* 2013; **35**(3): 611–23.  
**PubMed Abstract** | **Publisher Full Text** | **Free Full Text**
38. Rolls ET, Joliot M, Tzourio-Mazoyer N: **Implementation of a new parcellation of the orbitofrontal cortex in the automated anatomical labeling atlas.** *NeuroImage.* 2015; **122:** 1–5.  
**PubMed Abstract** | **Publisher Full Text**
39. Tzourio-Mazoyer N, Landau B, Papathanassiou D, et al.: **Automated anatomical labeling of activations in SPM using a macroscopic anatomical parcellation of the MNI MRI single-subject brain.** *NeuroImage.* 2002; **15**(1): 273–89.  
**PubMed Abstract** | **Publisher Full Text**
40. Joliot M, Jobard G, Naveau M, et al.: **AICHA: An atlas of intrinsic connectivity of homotopic areas.** *J Neurosci Methods.* 2015; **254:** 46–59.  
**PubMed Abstract** | **Publisher Full Text**
41. Fan L, Li H, Zhuo J, et al.: **The Human Brainnetome Atlas: A New Brain Atlas Based on Connectional Architecture.** *Cereb Cortex.* 2016; **26**(8): 3508–26.  
**PubMed Abstract** | **Publisher Full Text** | **Free Full Text**
42. Hammers A, Allom R, Koepf MJ, et al.: **Three-dimensional maximum probability atlas of the human brain, with particular reference to the temporal lobe.** *Hum Brain Mapp.* Wiley Online Library; 2003; **19**(4): 224–47.  
**PubMed Abstract** | **Publisher Full Text**
43. Yeo BT, Tandi J, Chee MW: **Functional connectivity during rested wakefulness predicts vulnerability to sleep deprivation.** *NeuroImage.* 2015; **111:** 147–158.  
**PubMed Abstract** | **Publisher Full Text**
44. Holmes AJ, Hollinshead MO, O'Keefe TM, et al.: **Brain Genomics Superstruct Project initial data release with structural, functional, and behavioral measures.** *Sci Data.* 2015; **2:** 150031.  
**PubMed Abstract** | **Publisher Full Text** | **Free Full Text**
45. Dickie EW, Ameis SH, Shahab S, et al.: **Personalized Intrinsic Network Topography Mapping and Functional Connectivity Deficits in Autism Spectrum Disorder.** *Biol Psychiatry.* 2018; **84**(4): 278–286.  
**PubMed Abstract** | **Publisher Full Text** | **Free Full Text**
46. Salehi M, Karbasi A, Shen X, et al.: **An exemplar-based approach to individualized parcellation reveals the need for sex specific functional networks.** *NeuroImage.* 2018; **170:** 54–67.  
**PubMed Abstract** | **Publisher Full Text** | **Free Full Text**
47. Dadi K, Abraham A, Rahim M, et al.: **Comparing functional connectivity based predictive models across datasets.** *2016 International Workshop on Pattern Recognition in Neuroimaging (PRNI).* 2016; 1–4.  
**Publisher Full Text**
48. Dadi K, Rahim M, Abraham A, et al.: **Benchmarking functional connectome-based predictive models for resting-state fMRI.** 2018.  
**Reference Source**
49. Urchs S, Armoza J, Benhajali Y, et al.: **MIST: A multi-resolution parcellation of functional networks.** *figshare.* Fileset. 2017.  
<http://www.doi.org/10.6084/m9.figshare.5633638.v1>
50. Fonov VS, Evans AC, McKinstry RC, et al.: **Unbiased nonlinear average age-appropriate brain templates from birth to adulthood.** *NeuroImage.* 2009; **47:** S102.  
**Publisher Full Text**

## Open Peer Review

Current Peer Review Status:

---

### Version 2

Reviewer Report 16 August 2019

<https://doi.org/10.21956/mniopenres.13872.r26151>

© 2019 Kelly C. This is an open access peer review report distributed under the terms of the [Creative Commons Attribution License](#), which permits unrestricted use, distribution, and reproduction in any medium, provided the original work is properly cited.



Clare Kelly

School of Psychology, Trinity College Institute of Neuroscience, Trinity College Dublin, Dublin, Ireland

The authors have comprehensively addressed my concerns.

**Competing Interests:** No competing interests were disclosed.

**I confirm that I have read this submission and believe that I have an appropriate level of expertise to confirm that it is of an acceptable scientific standard.**

Reviewer Report 05 March 2019

<https://doi.org/10.21956/mniopenres.13872.r26150>

© 2019 Uddin L. This is an open access peer review report distributed under the terms of the [Creative Commons Attribution License](#), which permits unrestricted use, distribution, and reproduction in any medium, provided the original work is properly cited.



Lucina Q. Uddin

Department of Psychology, Neuroscience Program, University of Miami, Miami, FL, USA

The authors have done a nice job addressing previous reviewer comments.

**Competing Interests:** No competing interests were disclosed.

**I confirm that I have read this submission and believe that I have an appropriate level of expertise to confirm that it is of an acceptable scientific standard.**

---

### Version 1

Reviewer Report 26 February 2018

<https://doi.org/10.21956/mniopenres.13827.r26070>

© 2018 Chyzyk D. This is an open access peer review report distributed under the terms of the [Creative Commons Attribution License](#), which permits unrestricted use, distribution, and reproduction in any medium, provided the original work is properly cited.



Darya Chyzyk 

Parietal team, INRIA, Paris-Saclay, Paris, France

There already exist many brain atlases based on anatomical or functional information and algorithms of the parcellation in the literature that was used for the atlas creation. This work presents an atlas from the date have been derived from resting-state fMRI data.

Sebastian Urchs, Pierre Bellec and colleagues present multi-resolution parcellation of the cortical, subcortical and cerebellar gray matter and reference to theoretical guarantees, Bootstrap Analysis of stable Clusters.

I truly liked this paper, it showed the importance of functional brain percolation and it practically use. The interactive web interface makes it possible to access to the different resolution of the atlas and directly incorporate to the brain analysis pipeline.

The strong point of the manuscript is the quality evaluation, which is very comprehensive. The parcellations stability was exterminated with functional homogeneity of the parcels and the comparison analysis with another commonly used atlases was presented.

Some notes for the minor revisions:

Could you please mention the previous version of the atlases and what are the crucial differences.

The number of the subjects selected for this atlas is limited to 190 subjects. Could you provide some discussion on

- importance of sample pool size in atlas generation
- prognosticate possible effect of larger number (~1000) of samples from GSP or UKBB datasets.

page 1, reference the NiLearn package and put the link to Nilearn and NIAK (page 3)

page 4, typo, 'the' appears 2 times in 'We used the the multi-scale stepwise'

page 15, figures 5 and 6. I'd suggest to make them more 'off-line friendly', indicating on the plot at least names of the atlases. These figures are very important and contain significant information, that is lost in the pdf format.

**Is the rationale for creating the dataset(s) clearly described?**

Yes

**Are the protocols appropriate and is the work technically sound?**

Yes

**Are sufficient details of methods and materials provided to allow replication by others?**

Yes

**Are the datasets clearly presented in a useable and accessible format?**

Yes

**Competing Interests:** No competing interests were disclosed.

**I confirm that I have read this submission and believe that I have an appropriate level of expertise to confirm that it is of an acceptable scientific standard.**

Author Response 04 Mar 2019

**Sebastian Urchs**, McGill University, Montreal, Canada

We thank Dr. Chyzhyk for her valuable feedback and suggestions. We respond below point by point (**our responses in bold**)

There already exist many brain atlases based on anatomical or functional information and algorithms of the parcellation in the literature that was used for the atlas creation. This work presents an atlas from the date have been derived from resting-state fMRI data.

Sebastian Urchs, Pierre Bellec and colleagues present multi-resolution parcellation of the cortical, subcortical and cerebellar gray matter and reference to theoretical guarantees, Bootstrap Analysis of stable Clusters.

I truly liked this paper, it showed the importance of functional brain percolation and its practical use. The interactive web interface makes it possible to access to the different resolution of the atlas and directly incorporate to the brain analysis pipeline.

The strong point of the manuscript is the quality evaluation, which is very comprehensive. The parcellations stability was demonstrated with functional homogeneity of the parcels and the comparison analysis with another commonly used atlases was presented.

Some notes for the minor revisions:

Could you please mention the previous version of the atlases and what are the crucial differences.

**We thank Dr. Chyzhyk for this comment. Indeed, the individual parcellations of the MIST parcellation have already been publicly available prior to this publication on figshare<sup>1</sup>. We have now added a section in the introduction highlighting this fact for users who have already been using this parcellation. We also point out that while the parcellations haven't changed from the previous version, we now have named and annotated them, and provide a data-derived hierarchical decomposition to facilitate their use, which is the core contribution of this work.**

The number of the subjects selected for this atlas is limited to 190 subjects. Could you provide some discussion on

- importance of sample pool size in atlas generation
- prognosticate possible effect of larger number (~1000) of samples from GSP or UKBB datasets.

**We have conducted a replication test of our original parcellation with the GSP dataset. We discuss the results of this analysis in a new section entitled "Generalizability of the parcellation". Overall, the agreement between the parcellations generated with the Cambridge and the GSP samples is good.**

page 1, reference the NiLearn package and put the link to NiLearn and NIAK (page 3)

page 4, typo, ‘the’ appears 2 times in ‘We used the the multi-scale stepwise’  
page 15, figures 5 and 6. I’d suggest to make them more ‘off-line friendly’, indicating on the plot at least names of the atlases. These figures are very important and contain significant information, that is lost in the pdf format.

**We thank Dr. Chyzyk for pointing out these mistakes in the original draft which we have corrected. We have addressed the shortcomings of the plotly-based interactive figures when viewed in the pdf version of the paper with the publisher. These figures now appear with static labels in the pdf version of the article.**

1.

[https://figshare.com/articles/Group\\_multiscale\\_functional\\_template\\_generated\\_with\\_BASC\\_on\\_the\\_C](https://figshare.com/articles/Group_multiscale_functional_template_generated_with_BASC_on_the_C)

**Competing Interests:** No competing interests were disclosed.

Reviewer Report 13 February 2018

<https://doi.org/10.21956/mniopenres.13827.r26051>

© 2018 Kelly C. This is an open access peer review report distributed under the terms of the [Creative Commons Attribution License](#), which permits unrestricted use, distribution, and reproduction in any medium, provided the original work is properly cited.



Clare Kelly

School of Psychology, Trinity College Institute of Neuroscience, Trinity College Dublin, Dublin, Ireland

The paper by Urchs *et al.* describes in careful detail the derivation and validation of a set of functional parcellation templates that identify hierarchical “functional building blocks” of the brain at different levels of resolution. The effort is notable for its (1) detailed description of the approach and methods, together with the open sharing of the data, code, and results – ensuring applicability and reproducibility, (2) inclusion of a systematic and meaningful parcel nomenclature, (3) attractive, effective, and visually appealing interactive viewer, which allows users to explore the hierarchical parcellations and provides a unique complement to the paper.

I have no comments on the methods or their implementation – these (e.g., NIAC, BASC) are well described and utilised in other papers. The MIST\_64 parcellation has been shown to perform well in a test of predictive models of a variety of disorders on the basis of functional connectivity data<sup>1</sup>.

My remarks primarily relate to the fact that there are many existing parcellations – indeed, the authors perform a relatively superficial quantitative comparison of these. What advantage does the current set of templates offer over existing ones? It would be useful to consider this directly in relation to some of the very widely used ones e.g., Yeo *et al.* (2011<sup>2</sup>; whose parcellation was based on a set of participants that likely included the ones who formed the basis of the current parcellation) and Glasser *et al.* (2016)<sup>3</sup>. The inclusion of subcortical areas including the cerebellum, for example, is a distinct advantage.

Second, perhaps the authors could offer some rationale as to why they selected a single sample of <200 participants from a single site as the dataset from which the templates would be derived. With such a

homogeneous sample and narrow age range, will the parcellations be widely applicable?

A particularly informative comparison/control employed by Craddock *et al.* 2011<sup>4</sup> was a “random” clustering based on mere spatial continuity. The “random” solutions performed surprisingly well. Employing such a comparison here might also strengthen the argument for the proposed template.

In the discussion of boundary/transition regions, a useful reference may be: Huntenburg, J. M., Bazin, P.-L., & Margulies, D. S. (2018). Large-Scale Gradients in Human Cortical Organization<sup>5</sup>.

## References

1. Dadi K, Abraham A, Rahim M, Thirion B, Varoquaux G: Comparing functional connectivity based predictive models across datasets. *International Workshop on Pattern Recognition in Neuroimaging*. 2016. 1-4
2. Yeo BT, Krienen FM, Sepulcre J, Sabuncu MR, Lashkari D, Hollinshead M, Roffman JL, Smoller JW, Zöllei L, Polimeni JR, Fischl B, Liu H, Buckner RL: The organization of the human cerebral cortex estimated by intrinsic functional connectivity. *J Neurophysiol*. 2011; **106** (3): 1125-65 [PubMed Abstract](#) | [Publisher Full Text](#)
3. Glasser M, Coalson T, Robinson E, Hacker C, Harwell J, Yacoub E, Ugurbil K, Andersson J, Beckmann C, Jenkinson M, Smith S, Van Essen D: A multi-modal parcellation of human cerebral cortex. *Nature*. 2016; **536** (7615): 171-178 [Publisher Full Text](#)
4. Craddock RC, James GA, Holtzheimer PE, Hu XP, Mayberg HS: A whole brain fMRI atlas generated via spatially constrained spectral clustering. *Hum Brain Mapp*. 2012; **33** (8): 1914-28 [PubMed Abstract](#) | [Publisher Full Text](#)
5. Huntenburg JM, Bazin PL, Margulies DS: Large-Scale Gradients in Human Cortical Organization. *Trends Cogn Sci*. 2018; **22** (1): 21-31 [PubMed Abstract](#) | [Publisher Full Text](#)

## Is the rationale for creating the dataset(s) clearly described?

Partly

## Are the protocols appropriate and is the work technically sound?

Yes

## Are sufficient details of methods and materials provided to allow replication by others?

Yes

## Are the datasets clearly presented in a useable and accessible format?

Yes

**Competing Interests:** No competing interests were disclosed.

**I confirm that I have read this submission and believe that I have an appropriate level of expertise to confirm that it is of an acceptable scientific standard, however I have significant reservations, as outlined above.**

Author Response 04 Mar 2019

**Sebastian Urchs**, McGill University, Montreal, Canada

We thank Dr. Kelly for her valuable feedback and suggestions that we have incorporated into the second version of this paper. We have addressed some specific comments below (**our responses in bold**).

The paper by Urchs et al. describes in careful detail the derivation and validation of a set of functional parcellation templates that identify hierarchical “functional building blocks” of the brain at different levels of resolution. The effort is notable for its (1) detailed description of the approach and methods, together with the open sharing of the data, code, and results – ensuring applicability and reproducibility, (2) inclusion of a systematic and meaningful parcel nomenclature, (3) attractive, effective, and visually appealing interactive viewer, which allows users to explore the hierarchical parcellations and provides a unique complement to the paper.

I have no comments on the methods or their implementation – these (e.g., NIAC, BASC) are well described and utilised in other papers. The MIST\_64 parcellation has been shown to perform well in a test of predictive models of a variety of disorders on the basis of functional connectivity data<sup>1</sup>. My remarks primarily relate to the fact that there are many existing parcellations – indeed, the authors perform a relatively superficial quantitative comparison of these. What advantage does the current set of templates offer over existing ones? It would be useful to consider this directly in relation to some of the very widely used ones e.g., Yeo et al. (2011<sup>2</sup>; whose parcellation was based on a set of participants that likely included the ones who formed the basis of the current parcellation) and Glasser et al. (2016<sup>3</sup>). The inclusion of subcortical areas including the cerebellum, for example, is a distinct advantage.

**We thank Dr. Kelly for these comments. In response, we have rewritten the abstract and introduction in order to clarify our rationale for developing a multi-resolution parcellation. We consider the multi-resolution decomposition and labels as the primary advantage of MIST over existing parcellations. As far as we know, there is no equivalent public data available. There are a few multiresolution atlases which include high resolution parcellations, e.g. [1,2], but they do not include or discuss network and sub-network decompositions. They also lack descriptive labels and don't match parcels across the resolutions. In the new version of this work, we have included an additional section entitled “Comparison to existing atlases” in which we discuss differences and commonalities with the Yeo and Glasser parcellations in more detail.**

Second, perhaps the authors could offer some rationale as to why they selected a single sample of <200 participants from a single site as the dataset from which the templates would be derived. With such a homogeneous sample and narrow age range, will the parcellations be widely applicable?

**In short, we selected a dataset that is (1) public and easy to access; (2) has typical characteristics; and, (3) has low motion levels. We have amended our description of the dataset with an explanation of this rationale. We also added a new section to the paper entitled “Generalizability” where we discuss an additional replication analysis of the MIST parcellation in two split-half samples of the original dataset and in an unrelated general population dataset. We discuss the results of this analysis in light of similar analyses in the existing parcellation literature. We have also included a discussion of a recent benchmark analysis by Dadi and colleagues [3] that show good performance of the MIST\_64 parcellation on machine learning applications. Overall, although the dataset used here is smaller than others used in the field, e.g. HCP, these results demonstrate that the robustness and quality of the MIST atlas match those of existing published atlases.**

A particularly informative comparison/control employed by Craddock et al. 20114 was a “random” clustering based on mere spatial continuity. The “random” solutions performed surprisingly well. Employing such a comparison here might also strengthen the argument for the proposed template. In the discussion of boundary/transition regions, a useful reference may be: Huntenburg, J. M., Bazin, P.-L., & Margulies, D. S. (2018). Large-Scale Gradients in Human Cortical Organization5.T

**We thank Dr. Kelly for this suggestion and have included the random parcels generated by Craddock et al. in our comparison of parcel homogeneity and illustrate our findings in the new section “Comparison with existing parcellations”. We find that the random Craddock parcels perform worse than connectivity-derived parcellations at lower spatial resolutions (generally larger parcel sizes) and begin outperforming connectivity-derived parcels at higher spatial resolutions (generally smaller parcel sizes). In general, we observe that differences in homogeneity between parcellations can almost entirely be explained by parcel size and intend to investigate this further in future work.**

1. Shen X, Tokoglu F, Papademetris X, Constable RT. Groupwise whole-brain parcellation from resting-state fMRI data for network node identification. *Neuroimage*. 2013;82: 403–415.
2. Craddock RC, James GA, Holtzheimer PE 3rd, Hu XP, Mayberg HS. A whole brain fMRI atlas generated via spatially constrained spectral clustering. *Hum Brain Mapp*. Wiley Subscription Services, Inc., A Wiley Company; 2012;33: 1914–1928.
3. Dadi K, Rahim M, Abraham A, Chyzhyk D, Milham M, Thirion B, et al. Benchmarking functional connectome-based predictive models for resting-state fMRI. 2018; Available: <https://hal.inria.fr/hal-01824205/>

**Competing Interests:** No competing interests were disclosed.

Reviewer Report 30 January 2018

<https://doi.org/10.21956/mniopenres.13827.r26049>

© 2018 Menon V. This is an open access peer review report distributed under the terms of the [Creative Commons Attribution License](#), which permits unrestricted use, distribution, and reproduction in any medium, provided the original work is properly cited.



### Vinod Menon

Department of Psychiatry and Behavioral Sciences, Symbolic Systems Program, Stanford University, Stanford, CA, USA

The methods and Toolbox provided by Urchs, Bellec and colleagues are an important contribution to the methods our field is developing for quantitative investigations of the brain function and structure. The Multiresolution resolution whole brain approach (including subcortical and cerebellar regions) and Bootstrap Analysis of Stable Clusters are important novel features of the study. I would have liked to see a replication analysis on HCP or NKI data to investigate correspondence - both convergence and divergence. A specific comparison with the Gasser parcellation would also have been helpful. Finally, I would suggest that code for the authors' study be distributed via Github to facilitate further improvements and testing.

**Is the rationale for creating the dataset(s) clearly described?**

Yes

**Are the protocols appropriate and is the work technically sound?**

Yes

**Are sufficient details of methods and materials provided to allow replication by others?**

Yes

**Are the datasets clearly presented in a useable and accessible format?**

Yes

**Competing Interests:** No competing interests were disclosed.

**I confirm that I have read this submission and believe that I have an appropriate level of expertise to confirm that it is of an acceptable scientific standard.**

Author Response 04 Mar 2019

**Sebastian Urchs**, McGill University, Montreal, Canada

We thank Dr. Menon for his valuable feedback and suggestions that we have incorporated into the second version of this paper. We have addressed some specific comments below (**our responses in bold**).

The methods and Toolbox provided by Urchs, Bellec and colleagues are an important contribution to the methods our field is developing for quantitative investigations of the brain function and structure. The Multiresolution resolution whole brain approach (including subcortical and cerebellar regions) and Bootstrap Analysis of Stable Clusters are important novel features of the study. I would have liked to see a replication analysis on HCP or NKI data to investigate correspondence - both convergence and divergence.

**We thank Dr. Menon for these comments. In response, we have conducted a replication analysis on the publicly available Genome Superstruct Project [1]. We chose this dataset over the HCP and NKI datasets suggested by Dr. Menon due to the similarity in acquisition parameters to the data we used in our original parcellation (3mm isotropic voxels, 2 second TR, interleaved acquisition) and that we believe still reflects a majority of the datasets used in the field. We discuss our findings regarding the replicability of the parcellations in the context of comparable analyses in the literature in a new section entitled “Generalizability of the parcellation”.**

A specific comparison with the Gasser parcellation would also have been helpful.

**We have added a new section entitled “Comparison with existing parcellations” where we discuss differences in the methodology and parcellation results with the Glasser and Yeo parcellations. In particular, we highlight the differences in approach and spatial coverage by with the Glasser parcels that make a quantitative comparison difficult.**

Finally, I would suggest that code for the authors' study be distributed via Github to facilitate further

improvements and testing.

**In addition to the public github repository for our interactive viewer ([https://github.com/SIMEXP/multiscale\\_dashboard](https://github.com/SIMEXP/multiscale_dashboard)), we have also released the code for our original parcellation and subsequent analyses in a second github repository ([https://github.com/surchs/MIST\\_atlas](https://github.com/surchs/MIST_atlas)).**

**1. Holmes AJ, Hollinshead MO, O'Keefe TM, Petrov VI, Fariello GR, Wald LL, et al. Brain Genomics Superstruct Project initial data release with structural, functional, and behavioral measures. *Sci Data*. 2015;2: 150031.**

**Competing Interests:** No competing interests were disclosed.

Reviewer Report 18 December 2017

<https://doi.org/10.21956/mniopenres.13827.r26052>

© 2017 Uddin L. This is an open access peer review report distributed under the terms of the [Creative Commons Attribution License](#), which permits unrestricted use, distribution, and reproduction in any medium, provided the original work is properly cited.



Lucina Q. Uddin

Department of Psychology, Neuroscience Program, University of Miami, Miami, FL, USA

The authors present results of a new parcellation method (MIST) based on resting state fMRI data. This is an elegant approach. Some suggestions and questions for clarification are below.

It is not immediately clear from the abstract why there is a need for yet another parcellation scheme, given multiple currently exist in the literature. Perhaps a line about what is novel and what limitations the current approach overcomes would help orient the reader right away.

Can the authors say more about why the particular dataset (Cambridge) was used in the current study? Other datasets with longer resting state fMRI scans collected at higher resolution exist (such as the Human Connectome Project). What was the rationale for choosing this particular dataset over others?

In general, how does the current work compare with parcellations that can be derived from ICA?

It may be worth mentioning in the discussion that other approaches for parcellation using resting state fMRI data have also been proposed:

[Development and validation of consensus clustering-based framework for brain segmentation using resting fMRI<sup>1</sup>](#).

## References

1. Ryali S, Chen T, Padmanabhan A, Cai W, Menon V: Development and validation of consensus clustering-based framework for brain segmentation using resting fMRI. *J Neurosci Methods*. 2015; **240**: 128-40 [PubMed Abstract](#) | [Publisher Full Text](#)

**Is the rationale for creating the dataset(s) clearly described?**

Partly

**Are the protocols appropriate and is the work technically sound?**

Yes

**Are sufficient details of methods and materials provided to allow replication by others?**

Yes

**Are the datasets clearly presented in a useable and accessible format?**

Yes

**Competing Interests:** No competing interests were disclosed.

**I confirm that I have read this submission and believe that I have an appropriate level of expertise to confirm that it is of an acceptable scientific standard, however I have significant reservations, as outlined above.**

Author Response 04 Mar 2019

**Sebastian Urchs**, McGill University, Montreal, Canada

We thank Dr. Uddin for her comments and feedback. Below we respond point by point (**our responses in bold**).

The authors present results of a new parcellation method (MIST) based on resting state fMRI data. This is an elegant approach. Some suggestions and questions for clarification are below. It is not immediately clear from the abstract why there is a need for yet another parcellation scheme, given multiple currently exist in the literature. Perhaps a line about what is novel and what limitations the current approach overcomes would help orient the reader right away.

**Thank you for the suggestion. We have rewritten the abstract and introduction to put more emphasis on (1) the multiresolution decompositions and (2) the multiresolution labels, which are to the best of our knowledge a new addition to the field. We have also added a section on the “Comparison with existing atlases” with a more in-depth discussion of related works.**

Can the authors say more about why the particular dataset (Cambridge) was used in the current study? Other datasets with longer resting state fMRI scans collected at higher resolution exist (such as the Human Connectome Project). What was the rationale for choosing this particular dataset over others?

**We have amended our description of the dataset to include the rationale for why we selected it. In brief, we have selected this dataset due to high quality of the imaging data, the low degree of motion and because the acquisition parameters (i.e. 2 second TR, 3mm isotropic voxels) are representative of the average imaging study in the field.**

In general, how does the current work compare with parcellations that can be derived from ICA?

It may be worth mentioning in the discussion that other approaches for parcellation using resting state fMRI data have also been proposed:

**We chose to restrict our quantitative evaluation to techniques which share the same objective of crisp parcellation, and not include linear decomposition which uncover gradients. We do agree that, in practice, there is a striking convergence between the two families of approaches, including for multiresolution decompositions, e.g. [1]. This will be a direction for future work.**

1. Jones DT, Vemuri P, Murphy MC, Gunter JL, Senjem ML, Machulda MM, et al. Non-stationarity in the “resting brain’s” modular architecture. *PLoS One*. 2012;7: e39731.

**Competing Interests:** No competing interests were disclosed.